frontiers in Earth Science

ORIGINAL RESEARCH
published: 15 November 2021
doi: 10.3389/feart.2021.772581

Lithofacies Types, Assemblage Characteristics, and Sedimentary Evolution Model of Lacustrine Shale in Dongyuemiao Formation of Fuxing Area

Yi Shu[1], Hanyong Bao[1], Youheng Zheng[1], Miankun Chen[1], Yongchao Lu[2], Haotian Liu[1], Wei Peng[1], Lin Zhou[1], Yiquan Ma[3], Yaru Wen[4], Qiming Wang[5] and Zhiyao Zhang[2]**

[1]Research Institute of Exploration and Development, Jianghan Oilfield Branch Company, Wuhan, China, [2]Key Laboratory of Tectonics and Petroleum Resources of Ministry of Education, China University of Geosciences, Wuhan, China, [3]Institute of Sedimentary Geology, Chengdu University of Technology, Chengdu, China, [4]Hubei Geological Survey, Wuhan, China, [5]Department of Earth and Environmental Sciences, The University of Texas at Arlington, Arlington, TX, United States

OPEN ACCESS

Edited by:
Shang Xu,
China University of Petroleum (East China), China

Reviewed by:
Rui Yang,
China University of Geosciences Wuhan, China
Chao Liang,
China University of Petroleum (Huadong), China

***Correspondence:**
Zhiyao Zhang
1075231995@qq.com
Qiming Wang
qiming.wang@mavs.uta.edu

Specialty section:
This article was submitted to Economic Geology, a section of the journal Frontiers in Earth Science

Received: *08 September 2021*
Accepted: *18 October 2021*
Published: *15 November 2021*

Citation:
Shu Y, Bao H, Zheng Y, Chen M, Lu Y, Liu H, Peng W, Zhou L, Ma Y, Wen Y, Wang Q and Zhang Z (2021) Lithofacies Types, Assemblage Characteristics, and Sedimentary Evolution Model of Lacustrine Shale in Dongyuemiao Formation of Fuxing Area. Front. Earth Sci. 9:772581. doi: 10.3389/feart.2021.772581

The identification and classification of lithofacies' types are very important activities in shale oil and gas exploration and development evaluation. There have been many studies on the classification of marine shale lithofacies, but research on lacustrine shale lithofacies is still in its infancy. Therefore, in this study, a high-resolution sequence stratigraphic framework is established for the lacustrine shale of the Jurassic Dongyuemiao Formation in the Fuxing area using detailed core observations, thin section identification, XRD analysis, major and trace element analysis, wavelet transform analysis, and detailed identification and characterization of the fossil shell layers in the formation. In addition, the lithofacies' types and assemblages are identified and characterized, and the lithofacies' characteristics and sedimentary evolution models in different sequence units are analyzed. The significance of the lithofacies assemblages for shale oil and gas exploration is also discussed. The results show that the shale of the target interval can be divided into 8 parasequence sets; further, 9 types of lithofacies and 6 types of lithofacies assemblages are identified. The 9 lithofacies are massive bioclast-containing limestone shoal facies (LF1), thick-layered fossil shell–containing limestone facies (LF2), layered mud-bearing fossil shell–containing limestone facies (LF3), laminated fossil shell–containing argillaceous shale facies (LF4), laminated fossil shell–bearing argillaceous shale facies (LF5), argillaceous shale facies (LF6), massive storm event–related bioclast-containing facies (LF7), massive argillaceous limestone facies (LF8), and massive mudstone facies (LF9). The sedimentary evolution models of different lithofacies are established as follows: Unit 1 (LF1-LF6) of the Dong-1 Member corresponds to the early stage of a lake transgressive system tract, and Units 2–4 (LF4-LF7) correspond to the middle to late stage of the lake transgressive system tract, which was an anoxic sedimentary environment. The Dong-2 Member (LF7-LF8) and the Dong-3 Member (LF5+LF9) correspond to a lake regressive system tract, which was an oxygen-rich sedimentary environment. Based on the characteristics of the shale lithofacies, sedimentary

environment, and the quality of the reservoir, the lithofacies assemblage of LF4–LF7 in Unit 4 is the most favorable type for oil and gas exploration, followed by the lithofacies assemblage in Unit 2; the lithofacies assemblage in the Dong-2 and Dong-3 Members are the worst.

Keywords: lithofacies (assemblages), shale oil, sedimentary evolution, dongyuemiao, sichuan basin

INTRODUCTION

Beginning in 2010, this research group began to study the potential for the exploration and development of shale oil and gas in China's geological terrain by drawing lessons from the successful shale revolution in the United States. In recent years, research on shale oil has become extremely important (Jia et al., 2013a; Sun et al., 2013; Xu et al., 2015; He et al., 2017; Wang et al., 2018; Li W. et al., 2020). At present, shale oil research in the United States is mainly focused on the Permian, Bakken, Eagle Ford, Niobrara, and other zones, and most of them are marine deposits. Recent exploration results in China show that the Songliao Basin and the Bohai Bay Basin in eastern China, the Ordos Basin and the Sichuan Basin in central China, and the tight oil and shale oil in the Jungar Basin and the Qaidam Basin in western China have good oil and gas exploration potential, and all of them mainly developed in lacustrine sedimentary environments. Compared with the marine shale in North America and the shale of the Wufeng–Longmaxi Formation in the Sichuan Basin in China, lacustrine shale has strong heterogeneity, high reservoir plasticity, and complex fluid properties. Due to the supply of sediments from multiple sources in different directions in the same period and the lateral migration of sedimentary centers in different periods, multiple types and multi-stage interlayers are developed in the shale; the temporal and spatial heterogeneity of shales' lithofacies is strong (Bohacs et al., 2000; Chamberlain et al., 2013; Desborough, 1978; Doebbert et al., 2010; Liu et al., 2018a; Ma et al., 2017; Zhang et al., 2017).

Shale oil is mainly divided into three types: the matrix type, interlayer type, and fracture type. Many scholars have studied lithofacies, sedimentary environment, and genetic model of different types of shale (Carroll and Bohacs, 2001; Lei et al., 2002; Meng et al., 2012; Zhang et al., 2012; Chamberlain et al., 2013; Strobl et al., 2014; Bruner et al., 2015; Lazar et al., 2015; Liu et al., 2018a; Deng et al., 2019). In terms of petrological research, comprehensive investigations have been carried out using core descriptions, thin section analysis, scanning electron microscopy, and X-ray diffraction analysis. At the same time, the heterogeneity of different types of shale lithofacies is reflected in its sedimentary structure (lamina and paleontology), organic matter content, and diagenesis (Surdam and Stanley, 1979; Bohacs et al., 2000; Loucks et al., 2007; Mitra et al., 2010; Xu et al., 2020a). Studies on the lacustrine shale of the Shahejie Formation in the Bohai Bay Basin have revealed that its lithofacies is divided into felsic shale, mixed shale, dolomite and carbonate shale, and massive, layered, and laminar shale (Ma et al., 2017; Bai et al., 2020; Li M. et al., 2020; Wu et al., 2020). In addition, studies on the sedimentary environment and genetic model of lacustrine organic-rich shales using sedimentology theory have shown that changes in the paleoclimate and tectonic activity are important factors controlling the evolution of ancient lake basins (Carroll and Bohacs, 1999; Sageman et al., 2003; Macquaker et al., 2010; Jia et al., 2013b; Egenhoff and Fishman 2013; Bruner et al., 2015; Ma et al., 2017; Liu et al., 2020; Gou et al., 2021); some scholars have also classified the lacustrine shale in the Sichuan Basin into pure shales deposited in a deep lake, shales intercalated with calcareous strips deposited in a shallow lake, and shales intercalated with thin fossil shell–containing limestone layers deposited in a semi deep lake.

In addition, many scholars have begun to pay attention to the significance of sedimentary structures, such as interlayers in organic-rich shale, for lithofacies identification and oil and gas exploration (Birdwell et al., 2016; Ougier-Simonin et al., 2016; Chen et al., 2017; Liang et al., 2017; Zou, 2017); much attention has been paid to carbonate interlayers commonly found in many continental lake basins, such as the Uinta Basin in the United States, the Cankiri–Corum Basin in Turkey, the Midland Valley Basin in Scotland, and the Bohai Bay Basin in eastern China, among others (Burton et al., 2014; Scherer et al., 2015; Merkel et al., 2016; Moradi et al., 2016; Liu et al., 2018b). Carbonate intercalations are deposited in shale as laminar or medium thick laminar, and their content and structure show obvious differences in the vertical direction (Hao et al., 2014; Bai et al., 2018; Liu H. et al., 2019; Zhang L. et al., 2019; Gou et al., 2019; Xu et al., 2020b). Many studies have also shown that total organic carbon (TOC) content, shale oil content, and reservoir quality play an important role in oil and gas accumulation; among these, the TOC content indicates the oil generation potential and the shale oil content, and shale porosity reflects the reservoir space characteristics (Katz, 2003; Kuhn et al., 2012; Holditch, 2013; Hao et al., 2014; Chen et al., 2017; Zou et al., 2019). The above indicators are closely related to the mineral composition, sedimentary structure, and petrological characteristics of shale. Therefore, the study of lacustrine shale lithofacies and lithofacies assemblages is of great significance to reveal the enrichment mechanism of shale oil and gas, and is also conducive to more effective shale oil and gas exploration and development (Birdwell et al., 2016; Liang et al., 2017; Zou, 2017; Shi et al., 2019a; Su et al., 2019).

Comprehensive research has shown that fine-detailed identification and description of lacustrine shale lithofacies is an important task for shale oil and gas exploration and development evaluation. At present, shale lithofacies are mostly divided based on mineral composition, sedimentary structure, and TOC content. However, research on the characteristics of shales with interlayers is obviously insufficient. For example, in the Jurassic Dongyuemiao

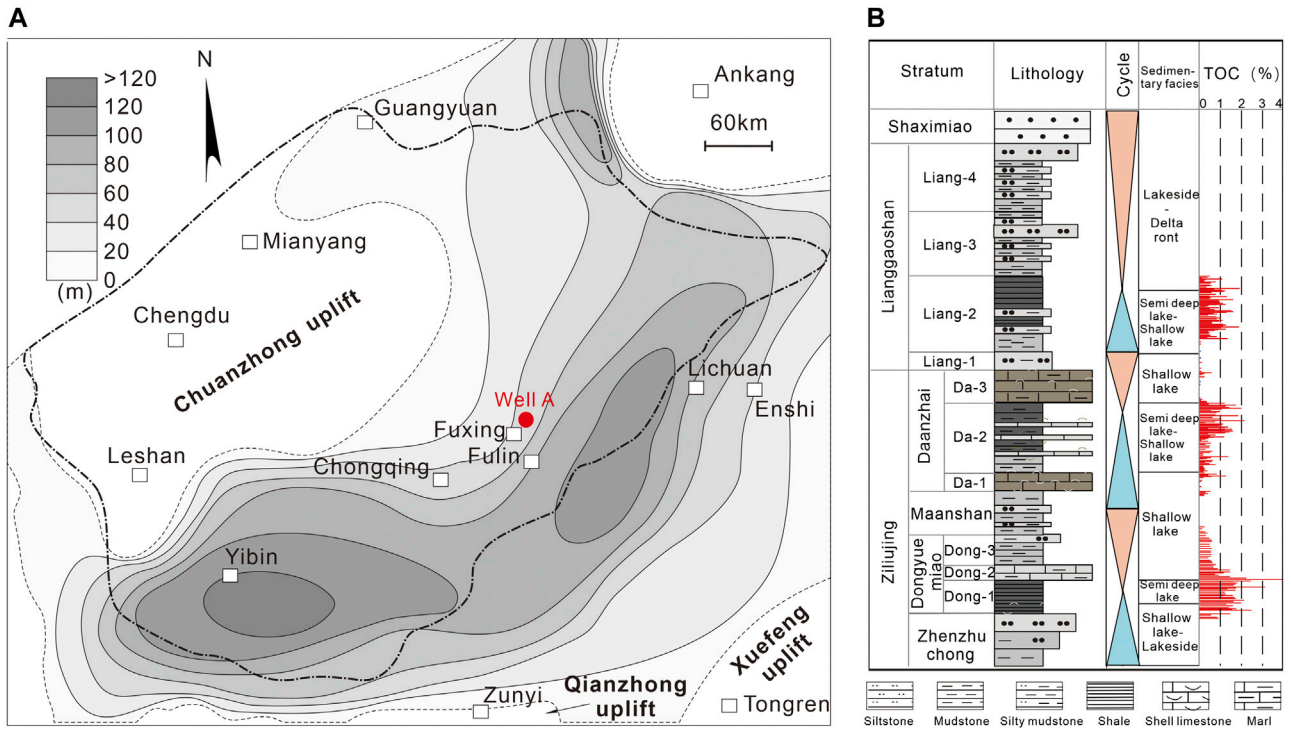

FIGURE 1 | (A) Location of the Fuxing area; **(B)** distribution diagram of Lower Jurassic strata in the Fuxing area.

Formation in the Sichuan Basin, the frequent development of fossil shell layers are of great significance for the exploration and development evaluation of the shale oil and gas in the area. This set of lacustrine shales, which are different from marine shales and the lacustrine shale in the Bohai Bay Basin, has high clay content, moderate thermal evolution (belonging to condensate oil and gas reservoirs), and many fossil shell interlayers. It is urgent to establish a lithofacies characterization scheme for this set of shale. In this study, Dong-1 Member is the key research object. Based on the establishment of a high-resolution sequence stratigraphic framework, mineralogical characteristics, sedimentary structure, fossil shell interlayer type, and organic carbon content, lithofacies characteristics of the shale and lithofacies assemblages are identified; in addition, the redox environment is analyzed, and the sedimentary evolution model of the different lithofacies assemblages and their significance for shale oil and gas exploration is discussed to provide a theoretical basis and technical support for the exploration and development of shale oil and gas in the Jurassic Dongyuemiao Formation in the Fuxing area.

GEOLOGICAL SETTING

The Fuxing area is located in the north of Sinopec mining right Qijiang–Fuling area. It is located in Chongqing, whose administrative division is subordinate to Liangping, Dianjiang, Fengdu, and Zhongxian. Structurally, it is located in the Wanxian syncline of the East Sichuan high and steep fold belt, with an area of 2,747 square kilometers. The area is a low mountainous to hilly landform that is 300–600 m above sea level and has convenient transportation and a well-developed water system. Since the end of the Middle Triassic, the Indosinian movement made the sea water to withdraw from the Sichuan Basin; the eastern edge of Loushan was connected to the ancient Jiangnan land and the basin entered an evolution stage of “circular depression” with deposition occurring in a lacustrine environment. Therefore, the sedimentary environment changed from a marine one to a lacustrine one. In the early Jurassic, the area of the lake basin’s center to the periphery was a half deep lake–deep lake, a shallow lake–half deep lake, a shore shallow lake, a shore lake, and a river environment. Jurassic strata in the Sichuan Basin are well developed. From the bottom to the top, they are the Lower Jurassic Ziliujing Formation, the Middle Jurassic Lianggaoshan Formation and the Shaximiao Formation, the Upper Jurassic Suining Formation, and the Penglaizhen Formation. The Lower Jurassic shale is mainly developed in the Dongyuemiao Formation, the Daanzhai Formation, the Lianggaoshan Formation, and the Ziliujing Formation (**Figure 1**). Controlled by tectonic subsidence, transgression, and regression, three sets of shallow lake to semi deep lake organic-rich shale are mainly deposited in the Lower Jurassic strata, among which good shale oil and gas exploration potential is seen in the Dong-1 Member, the Da-2 Member, and the Liang-2 Member.

METHODS

Wavelet Transform

Based on the theory of transgressive (T)–regressive (R) cycles and wavelet transform technology, in this study, a multi-scale analysis of the gamma logging curve was carried out through wavelet transform to establish a high-resolution sequence stratigraphy. The theoretical basis of the T-R cycle is that the rise and fall of the water level is the main controlling factor of sequence development; therefore, each water advance cycle and water retreat cycle are regarded as a complete sedimentary cycle (Guo et al., 1998; Wang, 2007; Du et al., 2016). Wavelet transform technology mainly uses the MATLAB software to process the gamma curve. The Morlet wavelet spectrum, which has been demonstrated to be effective in the periodic analysis of sedimentary cycles and sedimentary environments, was used with the value of the spectrum coefficient a being 256. After software processing, the wavelet analysis spectrum and the filtering analysis curve were obtained. The boundary and color depth of the energy mass in the wavelet analysis spectrum can effectively reflect the periodic characteristics of the sedimentary cycle. In this process, gamma logging data is replaced by the filtering analysis curve with certain periodicity, which is the basis of establishing the high-resolution sequence stratigraphy and identifying the sedimentary cycles (Li et al., 2009; Yang et al., 2019; Zhao et al., 2020).

TOC and XRD Analyses

To obtain the TOC content, the shale samples were treated with 200 mg powder to remove the carbonate content; the powder was treated with 10% hydrochloric acid at 60°C. Excess hydrochloric acid in the sample residue was removed using distilled water, and the samples were finally dried and TOC measurements were made using a CS844 Carbon/Sulfur Analyzer. For XRD analyses, the samples were scanned at a rate of 0.01°/s from angles of 2–70°at 20°C and a Bruker instrument was used for the analysis. All the measurements were done at the Petroleum Exploration and Development Laboratory, Jianghan Oilfield Branch Company, SINOPEC. Moreover, the analytical precision is better than 0.5% based on the Chinese National Standard GB/T 19145–2003.

Major and Trace Elements

The shale samples were treated to the powder and 50 mg powder was used for the analysis. First, the samples were pre-heated at 1,000°C for 90 min, and the weight change of the samples before and after pre-heating was recorded. Then the samples were mixed with 8x lithium tetraborate 186 ($Li_2B_4O_7$) to fuse them into glass beads. Second, they were wetted by a few drops of ultrapure water and a mixture of 1 ml hydrofluoric acid (HF) and 1 ml nitric acid (HNO_3) in a beaker. Then the beaker was sealed and placed in an oven and heated at 190°C for more than 48 h. Third, the slurry was evaporated at 115°C to near-dryness, and a mixture of 2 ml of HNO_3 and 3 ml of ultrapure water was added; then the beaker was sealed again to allow the residue to dissolve. Finally, the beaker was heated to 135°C for 5 h, and then the content was transferred to a polyethylene bottle and diluted to 100 ml with a mixture of 2% HNO_3. Then the sample was analyzed using an inductive coupled plasma–mass spectrometer (ICP-MS), with a precision of better than ±5%. The entire experiment was conducted at the ALS Chemex Laboratory (Guangzhou, China).

RESULTS

Sequence Stratigraphic Framework

The results of the Wavelet transform reveal that there are roughly three cycle combination modes: the combination mode in which the GR value increases upward is the water advance process, the combination mode in which the GR value decreases downward is the water retreat process, and the stable change of the GR value is the stable change stage of the horizontal plane. The logging data can effectively and accurately reflect the rhythmic sedimentary characteristics of the formation. The wavelet coefficient spectrum was obtained after processing by the wavelet transform technology. This method intuitively shows the mutation points and change areas between the frequency structure segments, and is displayed through the change in the local energy group and the periodic change characteristics. The corresponding relationship with the sequence framework at all levels can be established in turn. Compared with other logging data, the natural gamma ray (GR) curve is more sensitive to sand and mud content; after the wavelet exchange processing, the wavelet analysis map obtained can establish an effective relationship with the sequence framework. Based on the wavelet transform analysis of the FYA well in the Fuxing area and the T-R cycle theory, the target layer is divided into two system tracts (lacustrine transgressive system tract and lacustrine regressive system tract), and eight parasequence groups (8 Units) are identified; among these, the Dong-1 Member corresponds to Units 1–4, which reflect transgression overall; the Dong-2 Member corresponds to Unit 5, and the Dong-3 Member corresponds to Units 6–8. The Dong-2 and Dong-3 Members generally record a water regression (**Figure 2**).

Distribution Characteristics of Shell Fossils (Bioclasts) Interlayer

The observation of the core from the FYA well shows that laminated (< 0.01 m) fossil shell interlayers are commonly present in the Jurassic Dongyuemiao Formation in the Fuxing area (**Figure 3**; **Table 1**). The longitudinal distribution characteristics of fossil shell layers in the four parasequence formation units of the Dong-1 Member show obvious differences; in Unit 1, there are 126 laminae, 6 thin layers (0.01–0.1 m), and 4 medium layers (0.1–0.5 m) with fossils (bioclasts); in Unit 2, there are 214 laminae, 5 thin layers, and 2 layers with fossil shells; in Unit 3, there are 36 laminae, 10 thin layers, and 3 layers with fossil shells (bioclasts); and in Unit 4, there are 81 laminae and 7 thin layers with fossil shells (bioclasts). In the other parasequence sets, there are few layers with fossil shells (bioclasts). From the bottom to the top, the cumulative thickness of the fossil shell (bioclasts) layers in the four units of

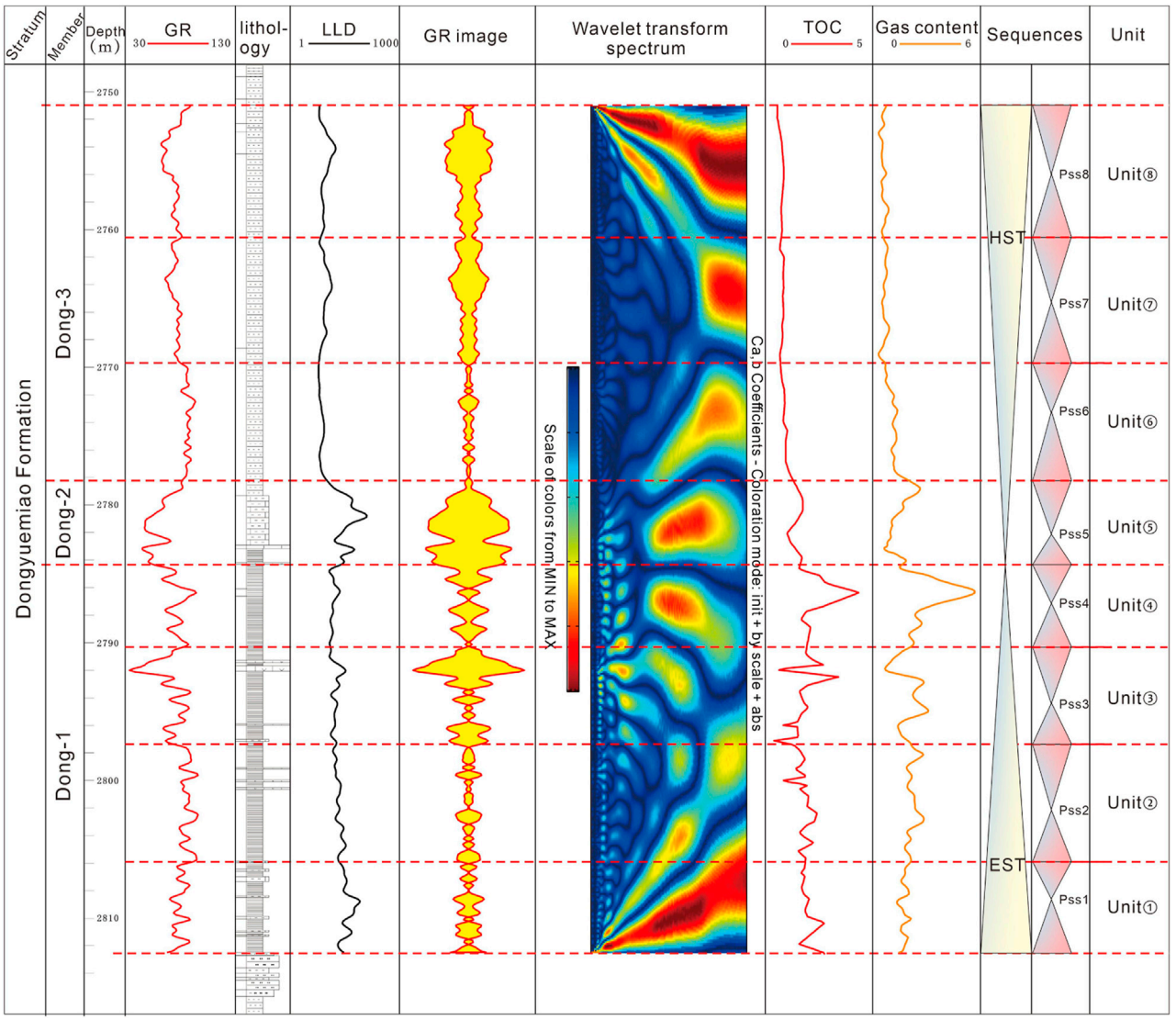

FIGURE 2 | Comprehensive histogram of high-resolution sequence stratigraphic division of FYA well in the Fuxing area.

the Dong-1 Member is 1.82, 0.74, 1.35, and 0.36 m, respectively. Among them, the number of laminar interlayers in Unit 2 and 4 is the largest. Compared with the other three units, the number of layers with bioclasts and the cumulative thickness of bioclast layers in Unit 4 are significantly reduced. In addition, comparing the TOC content of different units and the cumulative thickness of the fossil shell (bioclasts) layers shows that there is a certain positive correlation between them.

Petrologic Characteristics

XRD results show that the shale minerals in the Dongyuemiao Formation of the Fuxing area mainly include quartz, feldspar, carbonate, clay, pyrite, siderite, and other minerals. Among them, the content of clay minerals in shales of the Dong-1 Member accounts for 49.8–72.8%, with an average value of 64.3%, the carbonate content ranges from 0 to 30.7%, with an average of 4.38%, and the siliceous content accounts for 19.4–37.4%, with an average of 31.3%. The Dong-2 Member mainly contains limestones, and the carbonate minerals account for the largest proportion of minerals. The clay content in the Dong-3 Member is 35.8–68.2%, with an average value of 57.2%; the carbonate content is less, with an average of value 7.5%, and the siliceous content ranges from 29.0 to 44.7%, with an average of 35.2% (**Figure 4**). The XRD results and mineral ternary diagram analysis show that the samples of Units 1–4 and Unit 6 are mainly silty-rich mudstone, with a small amount of mixed mudstone, carbonate-rich mudstone, and carbonate mudstone; Unit 5 is mainly composed of carbonate mudstone; besides, the Unit 7 is mainly silty-rich mudstone and silty-rich/argillaceous mixed mudstone (**Figure 5**).

As one of the characteristics of shale, organic matter plays an important role in the exploration and development of shale oil

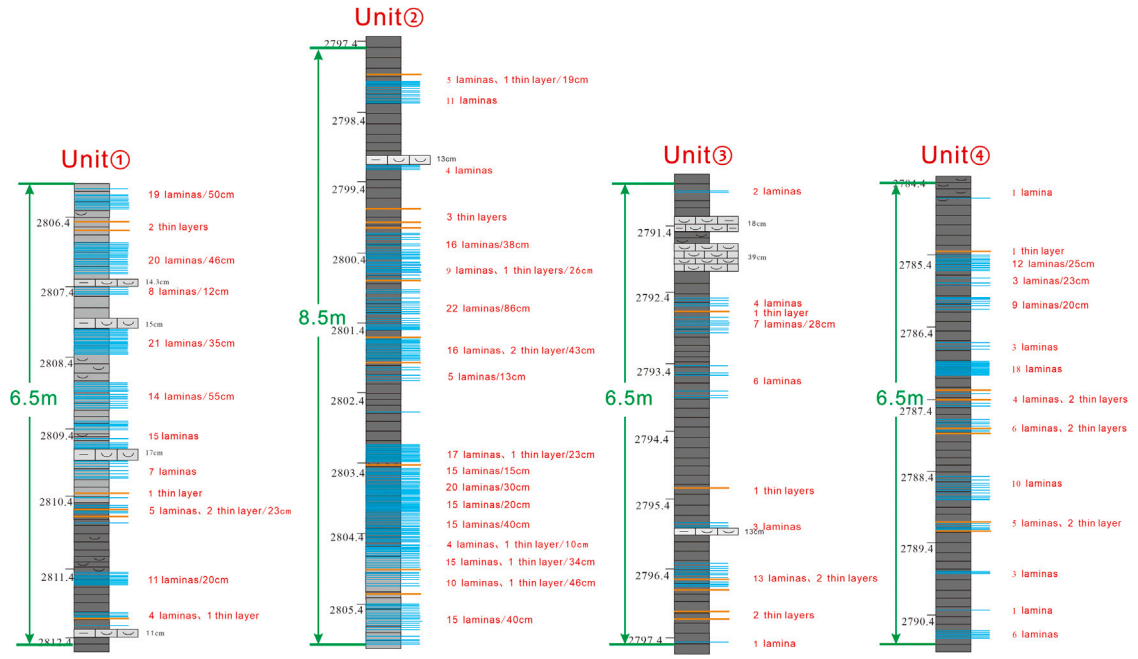

FIGURE 3 | Schematic diagram of development characteristics of shell fossils layer of the Dong-1 member of FYA well in the Fuxing area.

TABLE 1 | Statistical table of interlayer distribution in the East first member of Jurassic in the Fuxing area.

Interlayer type	Thickness (cm)	Unit①	Unit②	Unit③	Unit④
Middle layer	> 10	4	1	3	0
Thin layer	1–10	6	10	6	7
Lamina	< 1	126	214	36	81

and gas. Therefore, based on the division of lithofacies by the three terminal element diagram, the TOC content is included in the naming of lithofacies to effectively reflect the enrichment degree of organic matter in different lithofacies. Based on the TOC results, the lithofacies is divided into five grades: ≤0.5% (very low carbon), 0.5–1.0% (low carbon), 1.0–2.0% (medium carbon), 2.0–4.0% (high carbon), and >4% (rich carbon). A four-component lithofacies classification scheme is established based on the three-terminal member map of minerals (**Figure 6**).

Organic Geochemical Characteristics

From the bottom to the top, the TOC content generally shows a decreasing trend, but the Unit 4 section of the Dongyuemiao Formation has the highest range of TOC. Statistics show that the average TOC content of the four units in the Dong-1 Member is generally higher than that in the Dong-2 Member and the Dong-3 Member. The TOC content in the Dong-1 Member decreases first and then increases: Unit 4 (2.16 wt%) > Unit 1 (1.72 wt%) > Unit 2 (1.57 wt%) > Unit 3 (1.49 wt%). The average TOC content of the Dong-2 Member is 1.22 wt%, and the lowest TOC value of 0.55 wt% is in the Dong-3 Member (**Figure 7**).

As redox-sensitive elements, vanadium (V) and chromium (Cr) are widely used to indicate the redox environment during the deposition of paleowater (Algeo and Maynard, 2004; Algeo and Tribovillard, 2009; Liu et al., 2017; Lu et al., 2019; Ross and Bustin., 2009; Wang et al., 2018). The V/Cr ratio in the Dong-1 Member is higher than that in the Dong-2 Member and the Dong-3 Member; the V/Cr ratio in the Dong-1 Member is generally higher than 4.25, while in the Dong-2 Member and Dong-3 Member, the ratio is basically between 2–4.25, indicating that the sedimentary environment intensely changed upward from anoxic conditions to oxic conditions.

DISCUSSION

The Classification and Distribution of Lithofacies (Assemblages)

Observations of cores from the Dongyuemiao Formation in the Fuxing area show the presence of many fossil shell (bioclast) layers in the rock core. Through the detailed analysis of shell layers in different sequence units, nine lithofacies types are identified: bioclast-containing limestone shoal facies (LF1), thick-layered fossil shell–containing limestone facies (LF2), layered mud-bearing fossil shell–containing limestone facies (LF3), laminated fossil shell–containing argillaceous shale facies (LF4), laminated fossil shell–bearing argillaceous shale facies (LF5), argillaceous shale facies (LF6), massive storm event–related bioclast-containing facies (LF7), massive argillaceous limestone facies (LF8), and massive mudstone facies (LF9) (**Figure 8**). Among them, LF1 is mainly composed of light gray broken and clastic shell deposits, and

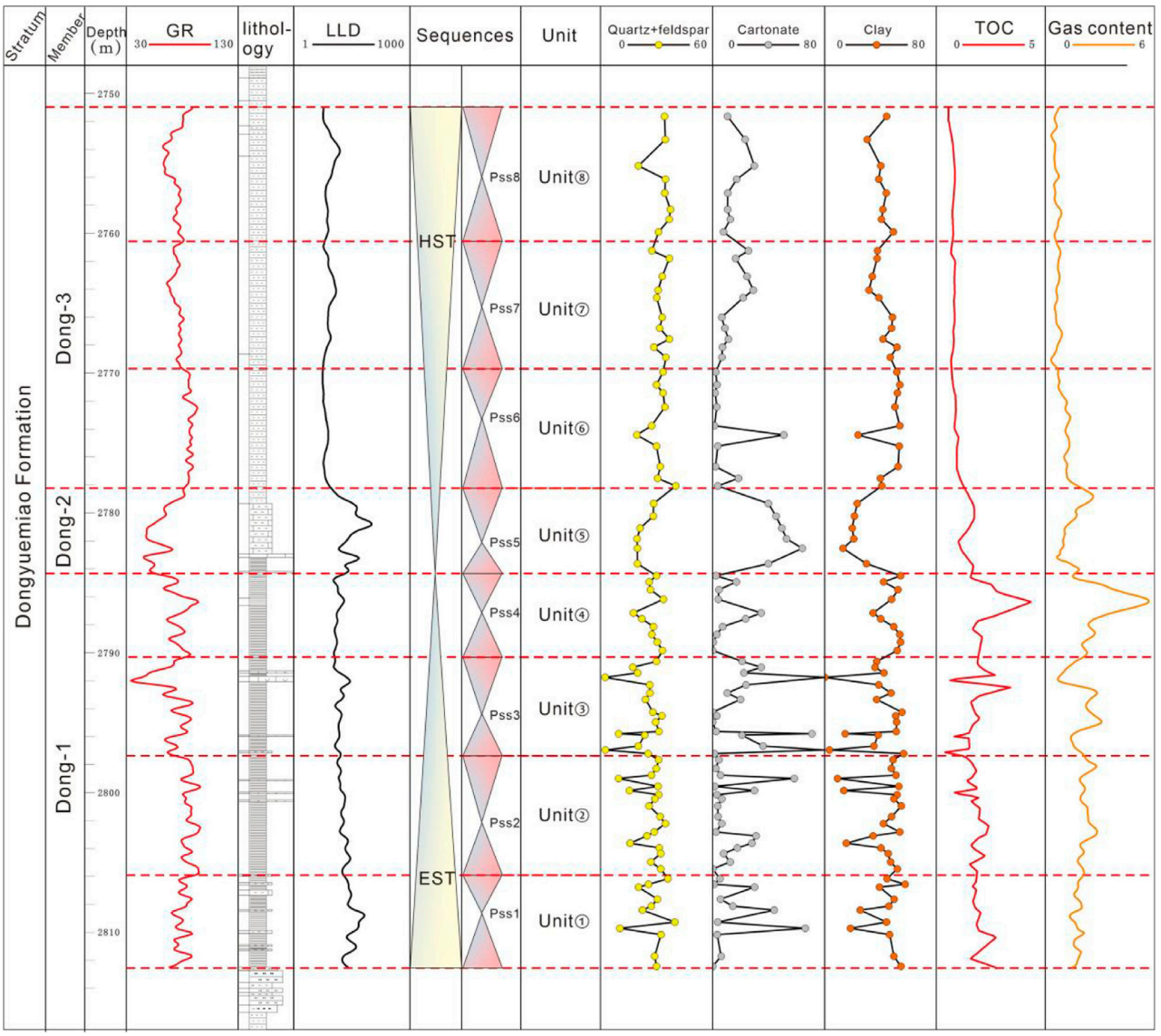

FIGURE 4 | Single well diagram of shale mineral components in the Dongyuemiao Formation of FYA well in the Fuxing area.

the shale content is less than 10%, with almost no intact shell seen. LF2 is a thick-layered fossil shell layer formed by the accumulation of a large number of shell organisms. It is mainly composed of relatively intact shell deposits and contains a small amount of medium-sized debris deposits. It has certain directionality, and the shale content is higher but generally less than 25%. LF3 is a medium to thin layer–containing fossil shells formed by the accumulation of shells and medium-sized debris. The overall preservation of the shells is relatively complete, and the content of the fossil shells accounts for 50–60%. Compared with LF2, the shale content is higher. LF4 is mainly a laminar deposit; the shells are relatively intact and appear as floating and laminar structures that are distributed in the black shale with a certain orientation; the proportion of shells is 30–50%. In LF5, the fossil shells are significantly reduced, but the fossil shells that are present are intact and appear as directional and floating structures; lamellae are distributed in the black shale, which contains almost no medium-sized debris; the shell content is less than 25%, and the matrix is composed of argillaceous shale. LF6 has foliation, is rich in organic matter, and contains almost no shell or debris. Massive fossil shell (bioclasts) deposits can be seen in LF7, and the shale content is generally less than 10%. The lithofacies has an obvious abrupt relationship with the upper and lower interfaces. There is no transitional lithology, and the maximum thickness is 55 cm, which is located at the top of Unit 3. LF8 is mainly distributed in the middle and upper part of Unit 5. The lithology is characterized by limestone, acid dropping, and violent bubbles. LF9 is mainly distributed in Units 6–8. The core is similar to the argillaceous shale of the

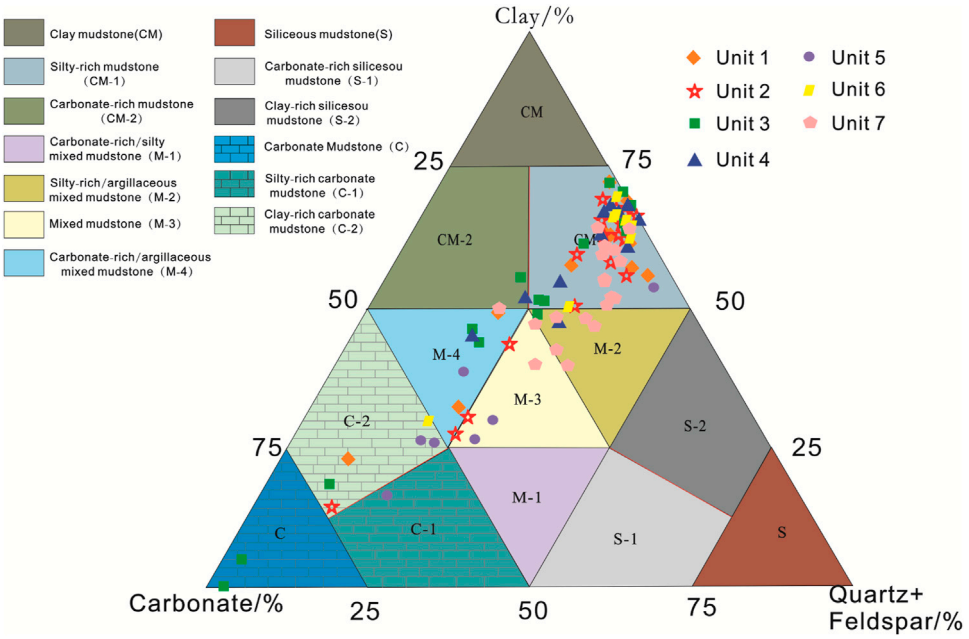

FIGURE 5 | Ternary diagram of mineral compositions in the Dongyuemiao Formation of FYA Well in the Fuxing area.

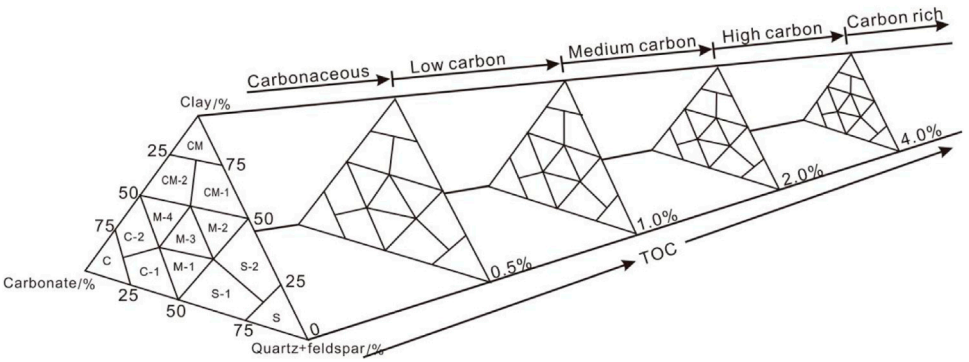

FIGURE 6 | Shale lithofacies division scheme of ternary diagram and TOC content in the Dongyuemiao Formation of FYA well in the Fuxing area.

Dong-1 Member, but the siliceous content is higher; most of the sediments in the core are also from terrigenous sources.

Based on the comprehensive analysis of the mineral ternary diagram, TOC content, and lithofacies type classification, six lithofacies assemblages are identified in shales of the Dongyuemiao Formation in the Fuxing area: LF1–LF6: it is mainly identified in Unit 1, and multi-stage transgressive and regressive cycle sequences can be identified from the bottom to the top; the transgressive lithofacies is characterized by the gradual change in the LF6-LF5-LF4-LF3-LF2-LF1 sequence, and the regressive cycle is characterized by the reverse change sequence of LF1-LF2-LF3-LF4-LF5-LF6 (**Figure 9**). LF4–LF7: it is mainly distributed in Units 2–3. The core observations show that the upper and lower argillaceous shale lithofacies are intercalated with medium and thin-layered storm event bioclast facies, with obvious lithologic interfaces and thickness of 1–13 cm. LF6–LF7: it is mainly located at the top of Unit 3 and has a thickness of 55 cm; storm event bioclast facies are intercalated with the argillaceous shale facies. LF4–LF7: it is identified in Unit 4 and is characterized by a high TOC content; the lithofacies assemblage is similar to LF2, but the difference is that the storm event bioclasts facies is mainly composed of thin-layered laminar sediments with a thickness of 1–5 cm. LF7–LF8: distributed in Unit 5, with a low TOC content and dominated by LF7 and LF8 deposits. LF5 + LF9: identified in Units 6–8, the TOC content is low, the LF9 type is mainly developed, and LF5 is occasionally seen (**Figure 10**).

Previous studies have shown that vanadium (V) and chromium (Cr) are easy to dissolve as redox-sensitive elements, which makes the concentration of these elements

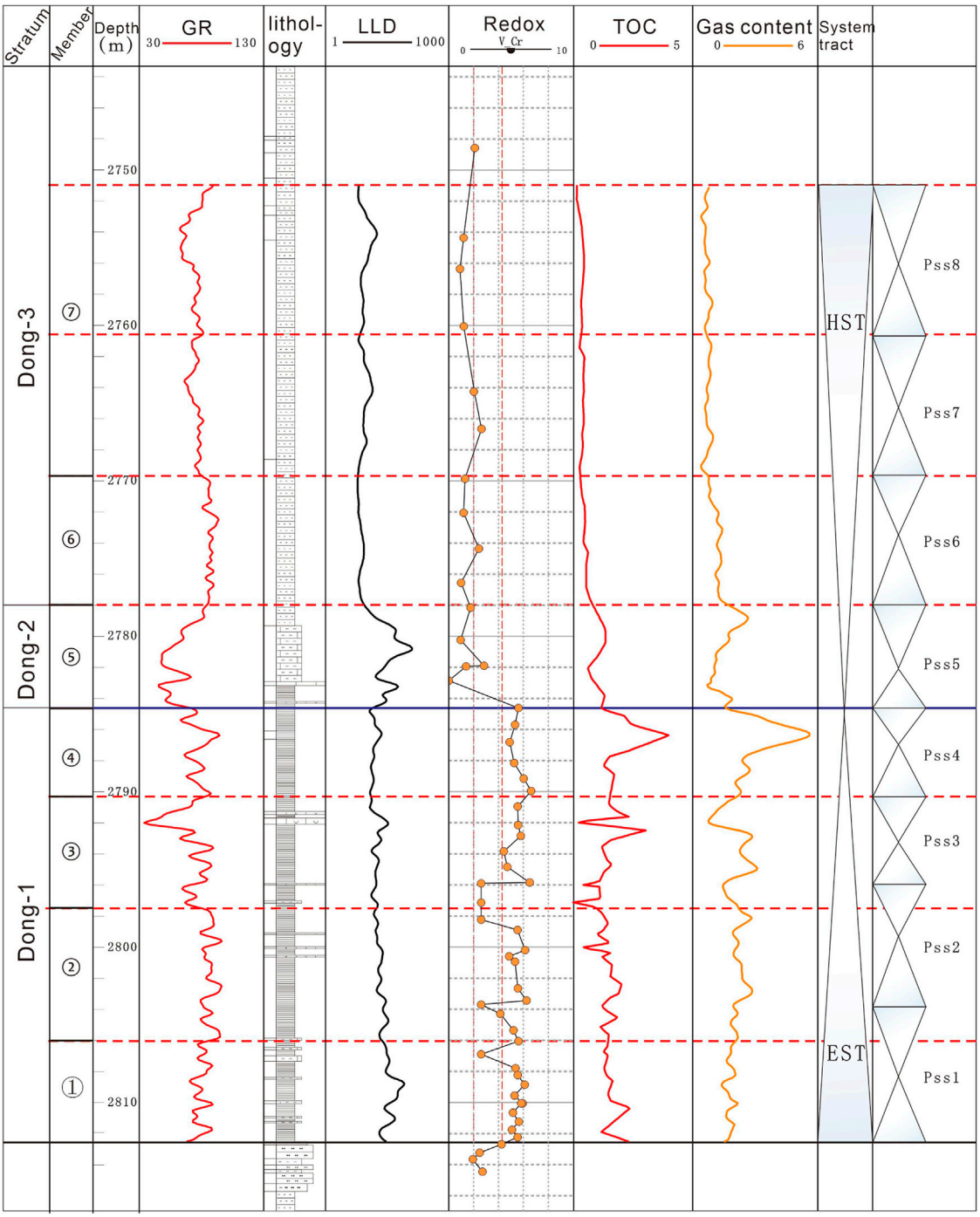

FIGURE 7 | Analysis of shale sedimentary environment of the Dongyuemiao Formation of FYA well in the Fuxing area.

low in oxidizing environments. On the contrary, in a reducing water environment, these elements are easily deposited and enriched due to their low solubility under anoxic conditions. When the V/Cr ratio > 4.25, it indicates an anoxic water environment; when it is between 2–4.25, it indicates a dysoxic sedimentary environment; and when it is < 2, it indicates an oxygen-rich sedimentary environment (Algeo and Maynard, 2004; Tribovillard et al., 2006; Wang et al., 2018; Lu et al., 2019). The V/Cr index of the shale samples from the Dongyuemiao Formation shows that the ratio is greater than 4.25 on the whole, which indicates that it was deposited in an anoxic sedimentary environment. Only individual shell layer samples show a dysoxic sedimentary environment. The results of shale samples from Dong-2 and Dong-3 Members show that

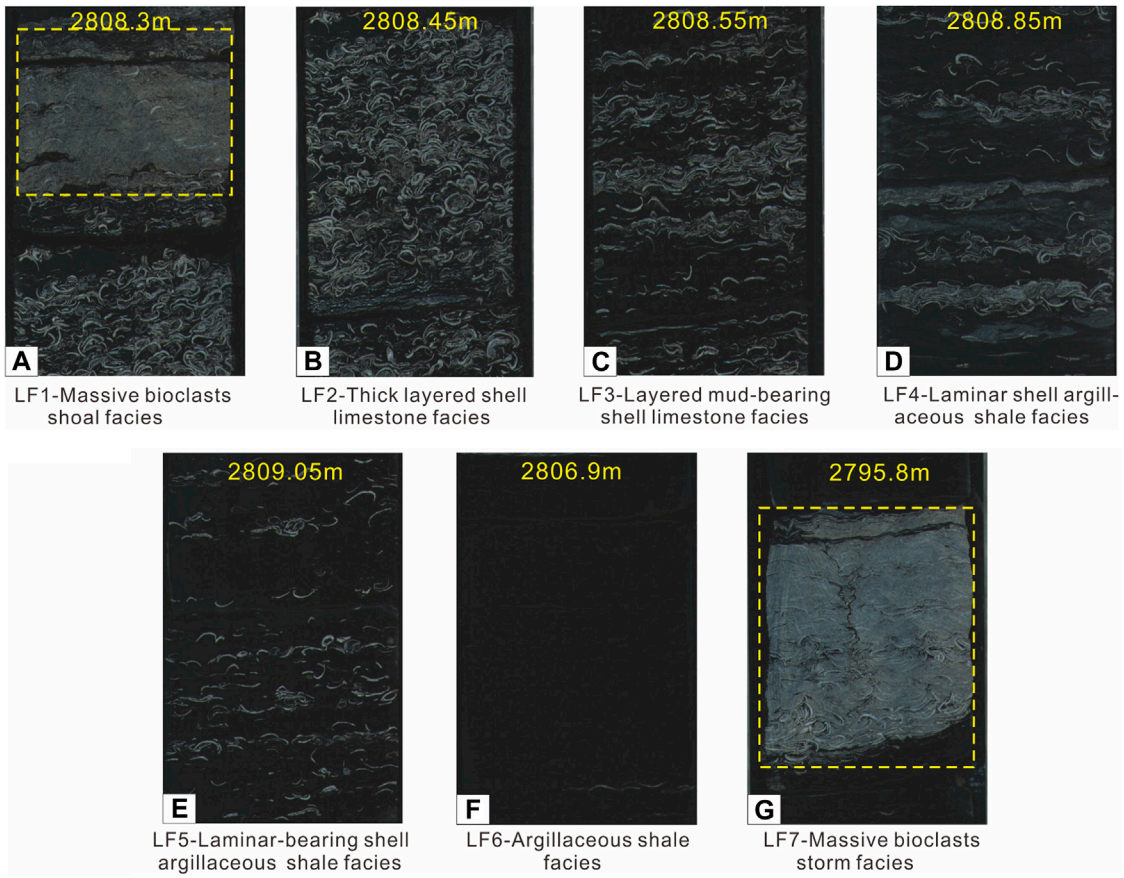

FIGURE 8 | Photos of seven lithofacies cores of FYA well in the Fuxing area.

the deposition in this period was basically in an oxygen-rich environment, reflecting the period from Dong-1 to Dong-3. Overall, the redox conditions show a trend of transformation to an oxidation environment, which further reveals the evolution trend of the shallower lake level.

Sedimentary Evolution Models of Different Lithofacies Assemblages

Under the influence of the sedimentary environment and lake level changes in different periods, the sedimentary models of the shale in different units of the Dongyuemiao Formation show great differences (Eugster and Surdam, 1973; Demaison and Moore, 1980; Jia et al., 2013b; Feng et al., 2016; Liu et al., 2018b; Shi et al., 2019b). Analysis of the characteristics and genesis of the lacustrine shale lithofacies assemblages in the Jurassic Dongyuemiao Formation in the Fuxing area show that the bottom-up lithofacies assemblage evolved from LF1–LF6 to LF5+LF9. Combined with redox environment analysis of this period, in the entire sedimentary cycle of the lake transgression and lake retreat, the lake basin evolved from a moist lake significantly affected by seasonal climate change to a dry lake that was shallower and not significantly affected by seasonal climate change. Finally, a sedimentary evolution model of the lacustrine shale lake in this area was established in this study; it can be divided into three evolution periods: the early stage of the lake transgressive system tract, the middle–late stage of the lake transgressive system tract, and the lacustrine regressive system tract (**Figure 11**).

In the early stage of the lake transgressive system tract, which corresponds to Unit 1, the LF1–LF6 assemblage was mainly developed, and multiple sets of transgressive and regressive sedimentary sequences can be seen from core observations, which are pointed out in Discussion 5.1 (**Figure 8**). In terms of lithology, the black shale is interbedded with laminated, thin, and medium–thick fossil shell layers with different thickness, and horizontal bedding is developed. The fossil shells in the core and thin section are complete in shape and different in size, and they are distributed in the black shale as layers or in suspension (**Figure 12B**). According to the analysis, it is considered that this lithofacies assemblage was mainly deposited in the lower part of a shallow lake and the middle-upper part of a semi deep lake located near the normal wave base, with strong hydrodynamic force. Under the dynamic action of waves, the complete shells passed through repeated panning and transformation, and finally formed the LF1 assemblage, which is a medium clastic beach sedimentary microfacies with broken shells. It is distributed in the lower part of the shallow lake sedimentary

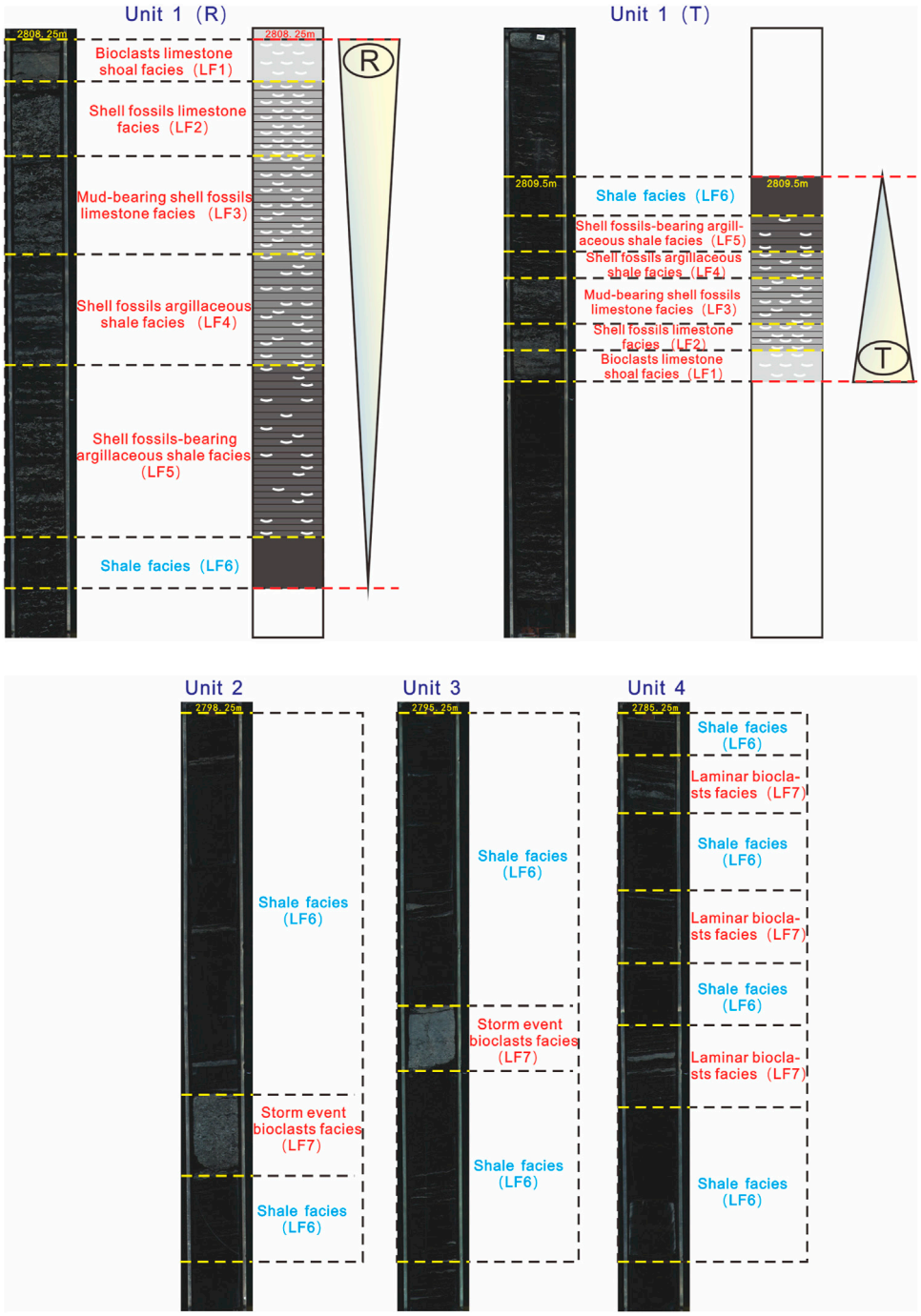

FIGURE 9 | Lithofacies distribution map of Dong-1 member of FYA well in the Fuxing area.

facies, and the content of mud is low (generally less than 10%). LF2–LF6 is mainly distributed in the semi deep lake sedimentary facies. As the lake water became deeper, the fossil shell content reduced and their preservation became better. LF6 is mainly deposited at the bottom of the semi-deep lacustrine facies (**Figure 11**). With the gradual rise of the lake level, the oxygen content in the bottom water of the lake decreased correspondingly. The redox index V/Cr ratio shows an upward trend from bottom to top.

Under the background of a humid paleoclimate, the rainfall was strengthened, which led to the injection of a large amount of freshwater carrying nutrients by fluvial action, and the lake level increased, entering the middle to late stage of the lake transgressive system tract and forming the largest lake

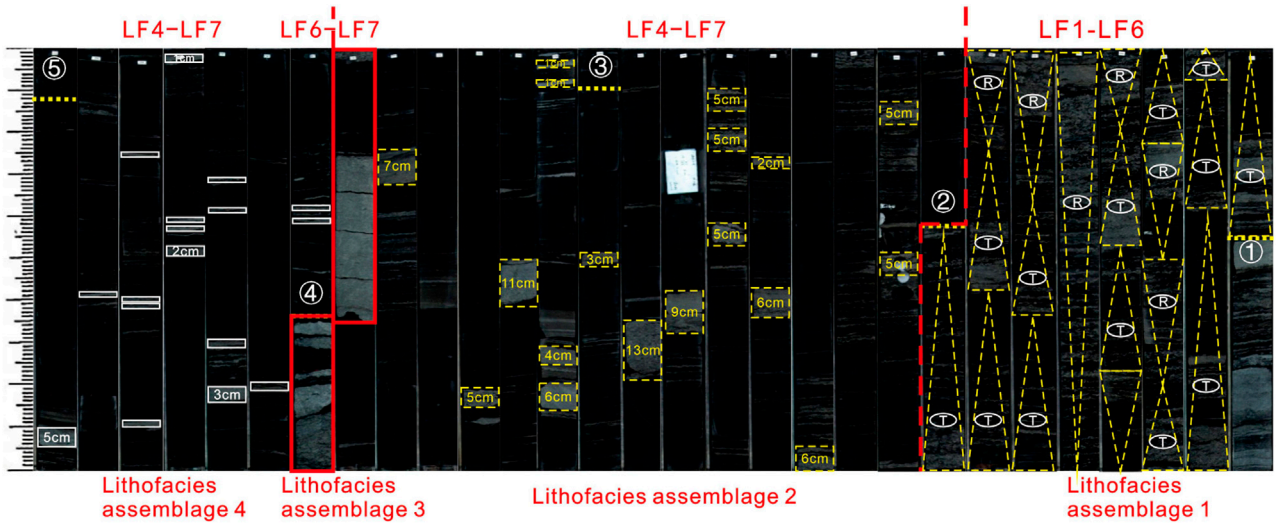

FIGURE 10 | Lithofacies assemblage division scheme of the Dong-1 member FYA well in the Fuxing area.

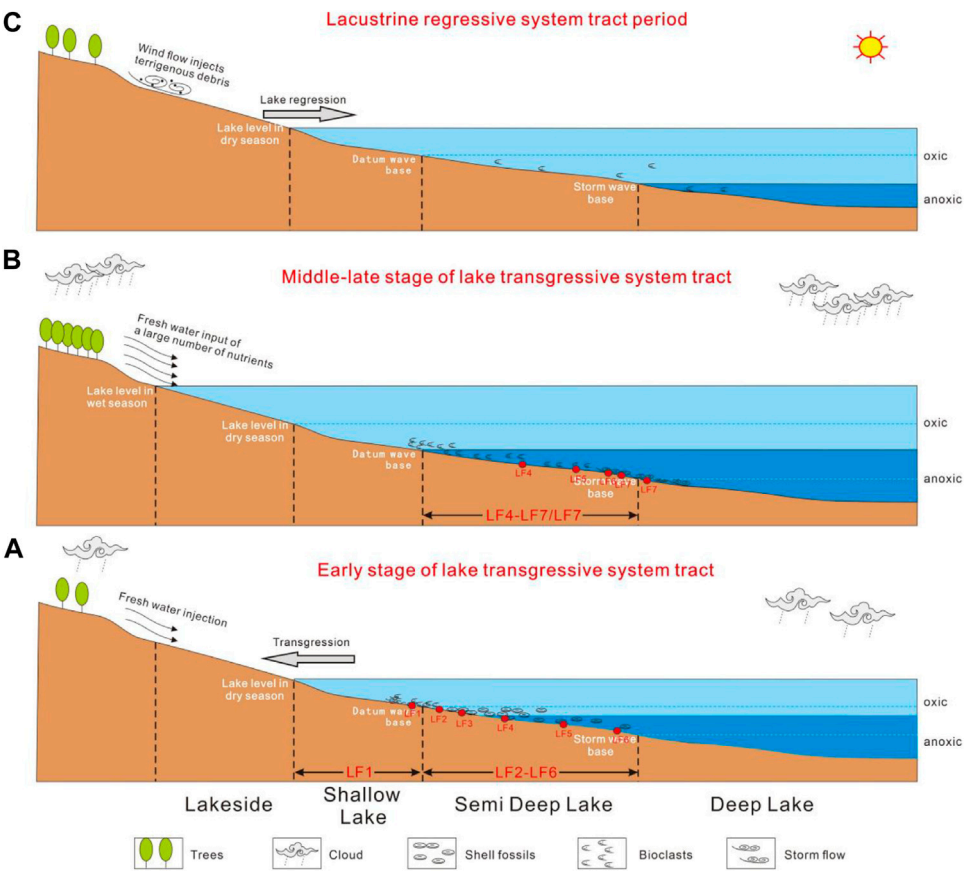

FIGURE 11 | Shale sedimentary evolution model diagram of the Jurassic Dongyuemiao Formation in the Fuxing area.

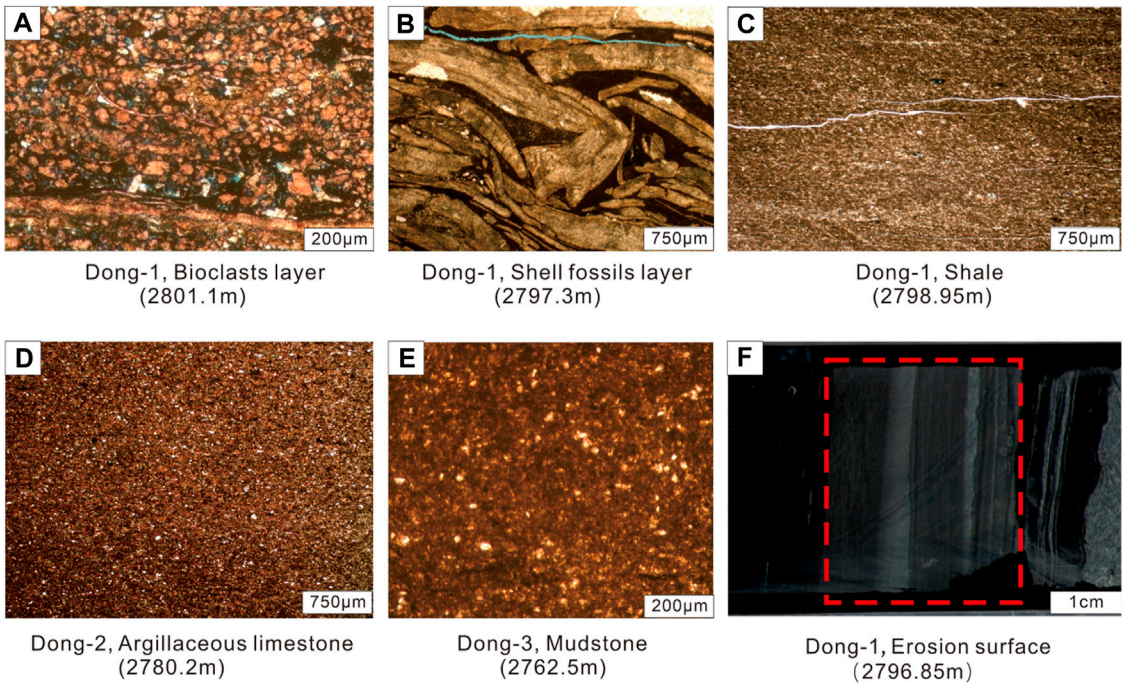

FIGURE 12 | Microscope photos of shale and core close-up of the Dongyuemiao Formation of FYA well in the Fuxing area.

flooding surface. In addition, the suitable paleoclimate and rainfall promoted the development of vegetation around the lake and blocked the injection of terrigenous debris transported by runoff; however, the transport of fine particles such as clay minerals and silty materials was enhanced due to the conservation of energy (Smith et al., 2014; Ma et al., 2020). This period roughly corresponds to Units 2–4 of the Dong-1 Member, of which Units 2–3 are mainly composed of the LF4–LF7 assemblage. In the core, there are two black shale segments intercalated with middle–thin gray bioclast layers, which were mainly deposited in the middle and lower part of a semi-deep lacustrine facies. There are multiple sets of bioclast layers with thicknesses between 5 and 25 cm. The individual shape of shells cannot be discerned, but the shell fragments can be seen in the thin sections (**Figure 12A**), and the shale content is less than 10%. Besides, this medium debris layer is in an unconformable contact with the upper and lower shale sections, which is different from Unit 1, and lacks a transitional lithofacies, reflecting the characteristics of event sedimentation. Combined with the geological background of this area, it is considered that LF7 is a storm deposition. Most of the fossil shells with complete morphology were formed into bioclast debris under the action of storm currents, and these are identified as storm beach sedimentary microfacies. The erosion surface structure can be seen in the lower part of most bioclast layers (**Figure 12F**). The sedimentary environment of this set of lithofacies assemblages is deeper than that of the lithofacies assemblage in Unit 1, and LF6 is a semi-deep lacustrine mud-containing sedimentary microfacies. In addition, a set of medium bioclast limestone sections with a thickness of about 55 cm is developed at the top of Unit 3. This set of thick-layered medium bioclast-containing limestone facies combined with the argillaceous shale facies (LF6) to form LF3, which is a semi-deep lake facies.

In Unit 4, the LF5–LF7 assemblage is developed, and the lithology is mainly black shale, which is obviously different from the deposits of layers containing fossil shells and bioclasts under the microscope, and the grain size is fine (**Figure 12C**). The lithofacies assemblage mainly consists of laminated bioclast layers with an accumulative thickness of 11.3 cm. There are 108 laminar bioclast-containing limestone interlayers with a density of 16.6/m. Compared with the lithofacies assemblage 2 in Units 2–3, the number of middle layers and thin bioclast-containing limestone interlayers is significantly reduced, and the thickness of a single layer and the cumulative thickness are obviously reduced. At this time, the maximum lake flooding surface was formed, and there was still storm flow at the bottom of the semi deep lake facies, but the intensity was weakened, the duration was reduced, and the location of the lithofacies deposition became deeper. In addition, imaging logging shows that the argillaceous shale facies and foliation are extremely developed (**Figure 13**), and that LF6 is a semi-deep lake mud microfacies. The analysis of sedimentary environment indicates an anoxic environment, which was beneficial to the generation and preservation of organic matter. After that, the indexes show a gradual downward trend, and the lake level also began to decrease, entering the period of the lacustrine regressive system tract.

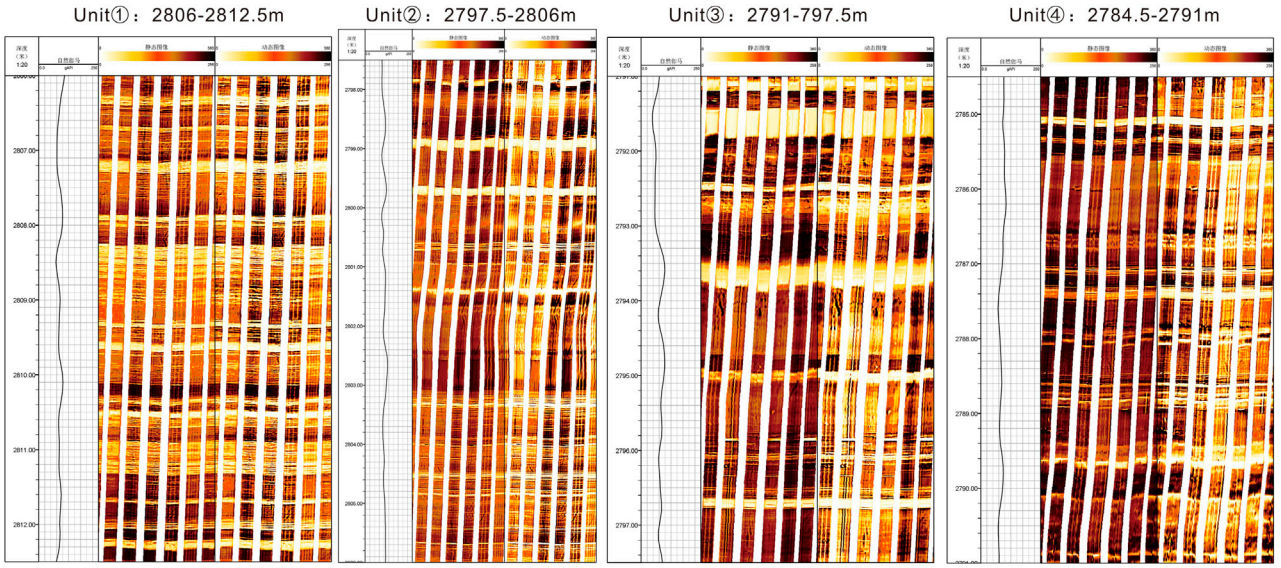

FIGURE 13 | Image logging maps of 4 units of the Dong-1 member of FYA well in the Fuxing area.

During the period of the lacustrine regressive system tract, with the decrease in the amount of rainfall, the paleoclimate was relatively arid. Due to the decrease in the input of fresh water into the lake, the lake level gradually decreased, and a certain amount of terrigenous debris entered the lake through eolian action. This period corresponds to the Dong-2 Member and the Dong-3 Member. The Dong-2 Member is mainly composed of LF7 and LF8 (**Figure 12D**), which is a carbon-bearing massive argillaceous limestone assemblage with fewer fossil shell layers and mainly shallow lake sediments. The lithology of the Dong-3 Member is dominated by black and grayish brown mudstone, and the LF5 and LF9 assemblages are developed (**Figure 12E**) with occasional bioclast layers. With the entry of terrigenous debris, the content of silty minerals and siliceous minerals increased and the TOC decreased as compared with the Dong-1 Member. The lake became shallower and the deposition during this time is mainly composed of shallow lake deposits. The redox index indicates that this period was in an oxidizing environment, and the total organic carbon content also shows a downward trend.

Significance of Different Lithofacies Assemblages for Shale Oil and Gas Exploration

Controlled by the sedimentary environment, there are obvious differences in lithofacies types and lithofacies assemblages in different units. On the premise of not being affected by external factors, different sedimentary environments determine the lithofacies assemblage characteristics of different strata in a basin (Abouelresh and slatt, 2012; Bai et al., 2020; Feng et al., 2016; Jin et al., 2006; Meng et al., 2012; Strobl et al., 2014; Yan and Zheng, 2015). Shale is the main hydrocarbon source rock in the study area, and the sedimentary environment during the shales' formation is conducive to the generation of oil and gas (Bai et al., 2020; Chen et al., 2017; He et al., 2017; Liang et al., 2018; Zhang S. et al., 2019); the later diagenetic process is also conducive to oil and gas accumulation (Ma et al., 2016; Yang et al., 2018). The shale of the Dongyuemiao Formation in the Fuxing area has multiple types of interlayers and strong heterogeneity, which indicates that not all the shale strata were involved in oil and gas accumulation. Therefore, the different lithofacies assemblage types played a vital role in oil and gas accumulation. Besides, the strong adsorption of clay minerals is conducive to the enrichment of organic matter (Bai et al., 2020; Ilgen et al., 2017) since shale oil and gas are stored in the micro and nano pores of shale through the adsorption of clay minerals. In addition to good hydrocarbon generation capacity, favorable migration channels and the reservoir space also affect the enrichment of shale oil and gas (Cancino et al., 2017; Elert et al., 2015; Zhang L. et al., 2019). According to the characteristics of the shale lithofacies in the Jurassic Dongyuemiao Formation in the study area, the LF1–LF6 lithofacies assemblage is mainly developed in Unit 1. The LF4–LF7 assemblage is developed in both Unit 2 and Unit 3, but there is a set of 55 cm thick layered medium bioclast limestone in Unit 3, which is distinguished from the lithofacies association type of Unit 2. Although LF4–LF7 assemblage is also developed in Unit 4, it is distinguished from the lithofacies assemblage of Unit 2 and Unit 3 by the presence of a thin laminar-stratified bioclast-containing interlayer. Since the TOC content, shale oil content, and reservoir quality are of great significance to oil and gas accumulation (Hao et al., 2014; Holditch, 2013; Katz, 2003; Kuhn et al., 2012; Zou et al., 2019), the TOC, physical properties, and oil and gas characteristics of the four units were compared (**Table 2**). Their ratings are as follow: Unit

TABLE 2 | Statistical table of key geological parameters of the Dong-1 member of FYA well in the Fuxing area.

Stratum		FYA						
Member	**Unit**	**Total Thickness (m)**	**Shell Thickness (m)**	**Shale Thickness (m)**	**TOC (%)**	**Porosity (%)**	**Gas Content (m^3/t)**	**Oil Content**
Dongyuemiao	④	6.5	0.32	6.18	2.12	6.41	2.89	6.06
	③	6.5	0.93	5.57	1.61	5.52	2.18	2.76
	②	8.5	0.67	7.83	1.82	5.30	2.18	2.31
	①	6.5	1.78	4.72	1.77	4.11	1.61	1.80

4 > Unit 2 > Unit 3 > Unit 1. Based on the above analysis and the sedimentary environment analysis, the four units of the Dong-1 Member were deposited in an anoxic sedimentary environment. Among them, the LF4–LF7 assemblage in Unit 4 is a favorable lithofacies assemblage type, with LF6 acting as a source rock, and LF4, LF5, and LF7 provide the reservoir space for oil and gas accumulation. Moreover, thin layer and laminar interlayers are favorable, while the massive mesoclastic interlayer is unfavorable for the migration and enrichment of oil and gas because of its massive structure (Li et al., 2017; Liu Z. et al., 2019; Zhang S. et al., 2019; Bai et al., 2020). Compared with Unit 2 and 3, Unit 4 has significantly less intermediate bioclast interlayers deposited by storm events, suggesting that the strong hydrodynamic effect of storm action is unfavorable for the enrichment and preservation of organic matter. The shale quality of Unit 3 is worse than that of Unit 2 due to the development of the 55 cm thick-layered bioclast-containing limestone. Besides, the lithofacies assemblage type of Unit 1 reveals that the frequent changes of the horizontal plane in this period and the LF1–LF3 assemblage are also not conducive to the enrichment of organic matter. Therefore, even if they have similar source rock conditions as Unit 4, their shale quality is slightly worse than that of Unit 4. The Dong-2 and Dong-3 Members were deposited in an oxygen-rich sedimentary environment, and their source rock conditions are obviously worse than those of the Dong-1 Member. Thus, the LF4–LF7 assemblage in Unit 4 of the Jurassic Dongyuemiao Formation in the Fuxing area is a favorable lithofacies association type for oil and gas accumulation, followed by Unit 2.

CONCLUSION

To clarify the shale lithofacies characteristics and sedimentary evolution of the Jurassic Dongyuemiao Formation in the Fuxing area, a high-resolution sequence stratigraphic framework was established using detailed descriptions of the core from the FYA well, wavelet transform analysis, XRD analysis, major and trace element analysis, TOC content analysis, sedimentary modeling, and other technical means. The lithofacies and lithofacies assemblages in the study area are identified and the sedimentary evolution model of different units is analyzed. The main conclusions are as follows:

1) Using the transgressive–regressive cycle theory and wavelet transform technology, a high-resolution sequence stratigraphic model of the strata of the Jurassic Dongyuemiao Formation in the Fuxing area is established. The target strata are divided into two system tracts—a lacustrine transgressive system tract and a lacustrine regressive system tract—and eight parasequence groups are identified. The Dong-1 Member represents the lacustrine transgressive system tract and includes four parasequence groups. The Dong-2 and Dong-3 Members represent lacustrine regressive system tracts and include 1 and 3 parasequence groups, respectively;
2) Through the detailed characterization of the layers containing fossil shells (bioclasts) in target strata in the area, the following facies are identified: massive bioclast-containing limestone shoal facies (LF1), thick-layered fossil shell–containing limestone facies (LF2), layered mud-bearing fossil shell–containing limestone facies (LF3), laminated fossil shell–containing argillaceous shale facies (LF4), laminated fossil shell–bearing argillaceous shale facies (LF5), argillaceous shale facies (LF6), massive storm event–related bioclast-containing facies (LF7), massive argillaceous limestone facies (LF8), and massive mudstone facies (LF9). In addition, based on the three-step lithofacies classification methods of whole rock mineral zoning, TOC classification, and sedimentary structure, six lithofacies assemblages are identified: LF1–LF6 (Unit 1), LF4–LF7 (Unit 2), LF6–LF7 (Unit 3), LF4–LF7 (Unit 4), LF7–LF8 (Unit 5), and LF5 + LF9 (Units 6–8);
3) Based on the analysis of lithofacies characteristics, genesis, and sedimentary environment, the evolution model of the shale of the Jurassic Dongyuemiao Formation in the Fuxing area is established; the model contains three periods: the Dong-1 Member corresponds to a lake transgressive system tract, which is an anoxic sedimentary environment and in which the depositional period of Unit 1 corresponds to the early stage of the lake transgressive system tract and Units 2–4 correspond to the middle–late stage of the lake transgressive system tract. The Dong-2 and Dong-3 Members correspond to the lake regressive system tract, which is an oxygen-enriched sedimentary environment. In addition, Unit 4 of the Dong-1 Member has high TOC, high porosity, and high gas content. The LF4–LF7 assemblage deposited during this sedimentation period is the most favorable lithofacies assemblage type for oil and gas accumulation.

DATA AVAILABILITY STATEMENT

The original contributions presented in the study are included in the article/Supplementary Material; further inquiries can be directed to the corresponding authors.

AUTHOR CONTRIBUTIONS

YS: writing—reviewing and editing. HB and MC: conceptualization, methodology, and software. YL: supervision. HL, WP, LZ, and YM: visualization and investigation. QW and ZZ: visualization and investigation.

FUNDING

The study was funded by the NSFC (National Natural Science Foundation of China) (No. 41802175) and Natural Science Foundation of Hubei Province (No. 2020CFB501).

ACKNOWLEDGMENTS

We appreciate the core and data access provided by the Jianghan Oilfield Branch Company, Sinopec; the team members of the Jianghan Oilfield Branch Company, Sinopec for their basic exploration work. We are particularly grateful to Professor Xu Shang for his critical and constructive comments.

REFERENCES

Abouelresh, M. O., and Slatt, R. M. (2012). Lithofacies and Sequence Stratigraphy of the Barnett Shale in East-central Fort Worth Basin, Texas. *Bulletin* 96 (1), 1–22. doi:10.1306/04261110116

Algeo, T. J., and Maynard, J. B. (2004). Trace-element Behavior and Redox Facies in Core Shales of Upper Pennsylvanian Kansas-type Cyclothems. *Chem. Geol.* 206 (3–4), 289–318. doi:10.1016/j.chemgeo.2003.12.009

Algeo, T. J., and Tribovillard, N. (2009). Environmental Analysis of Paleoceanographic Systems Based on Molybdenum–Uranium Covariation. *Chem. Geol.* 268 (3–4), 211–225. doi:10.1016/j.chemgeo.2009.09.001

Bai, C., Yu, B., Han, S., and Shen, Z. (2020). Characterization of Lithofacies in Shale Oil Reservoirs of a Lacustrine basin in Eastern China: Implications for Oil Accumulation. *J. Pet. Sci. Eng.* 195, 107907. doi:10.1016/j.petrol.2020.107907

Bai, C., Yu, B., Liu, H., Xie, Z., Han, S., Zhang, L., et al. (2018). The Genesis and Evolution of Carbonate Minerals in Shale Oil Formations from Dongying Depression, Bohai Bay Basin, China. *Int. J. Coal Geology.* 189, 8–26. doi:10.1016/j.coal.2018.02.008

Birdwell, J. E., Berg, M. D. V., Johnson, R. C., Mercier, T. J., Boehlke, A, and Brownfield, M. E. (2016). *Geological, Geochemical and Reservoir Characterization of the Uteland Butte Member of the Green River Formation*. Utah: Uinta Basin.

Bohacs, K. M., Carroll, A. R., and Neal, J. E. (2000). Lake-basin Type, Source Potential, and Hydrocarbon Character: an Integrated Sequence-Stratigraphic Geochemical Framework (In lake Basins through Space and Time). *AAPG* 83, 143–162.

Bruner, K. R., Walker-Milani, M., and Smosna, R. (2015). Lithofacies of the Devonian Marcellus Shale in the Eastern Appalachian Basin, U.S.A. *J. Sediment. Res.* 85 (8), 937–954. doi:10.2110/jsr.2015.62

Burton, D., Woolf, K., and Sullivan, B. (2014). Lacustrine Depositional Environments in the Green River Formation, Uinta Basin: Expression in Outcrop and Wireline Logs. *Bulletin* 98 (9), 1699–1715. doi:10.1306/03201413187

Carroll, A. R., and Bohacs, K. M. (2001). Lake Type Controls onPetroleum Source Rock Potential in Nonmarine Basins. *AAPG Bull.* 85 (6), 1033–1053. doi:10.1306/8626ca5f-173b-11d7-8645000102c1865d

Carroll, A. R., and Bohacs, K. M. (1999). Stratigraphic Classification of Ancient Lakes: Balancing Tectonic and Climatic Controls. *Geol* 27 (2), 99–102. doi:10.1130/0091-7613(1999)027<0099:scoalb>2.3.co;2

Chamberlain, C. P., Wan, X., Graham, S. A., Carroll, A. R., Doebbert, A. C., Sageman, B. B., et al. (2013). Stable Isotopic Evidence for Climate and Basin Evolution of the Late Cretaceous Songliao Basin, China. *Palaeogeogr. Palaeoclimatol. Palaeoecol.* 385, 106–124. doi:10.1016/j.palaeo.2012.03.020

Chen, Z., Li, M., Cao, T., Ma, X., Li, Z., Jiang, Q., et al. (2017). Hydrocarbon Generation Kinetics of a Heterogeneous Source Rock System: Example from the Lacsutrine Eocene-Oligocene Shahejie Formation, Bohai Bay Basin, China. *Energy Fuels* 31 (12), 13291–13304. doi:10.1021/acs.energyfuels.7b02361

Demaison, G. J., and Moore, G. T. (1980). Anoxic Environments and Oil Source Bed Genesis. *Org. Geochem.* 2, 9–31. doi:10.1016/0146-6380(80)90017-0

Deng, Y., Pu, X. G., Chen, S. Y., Yan, J. H., Shi, J. N., Zhang, W., et al. (2019). Characteristics and Controlling Factors of Fine Grained Mixed Sedimentary Rocks Reservoir: A Case Study of the 2nd Member of Kongdian Formation in Cangdong Depression, Bohai Bay Basin. *J. China Univ. Mining Tech.* 48 (6), 1301–1316. doi:10.13247/j.cnki.jcumt.001023

Desborough, G. A. (1978). A Biogenic-Chemical Stratified lake Model for the Origin of Oil Shale of the Green River Formation: an Alternative to the Playa-lake Model. *Geol. Soc. America Bull.* 89, 961–971. doi:10.1130/0016-7606(1978)89<961:abslmf>2.0.co;2

Doebbert, A. C., Carroll, A. R., Mulch, A., Chetel, L. M., and Chamberlain, C. P. (2010). Geomorphic Controls on Lacustrine Isotopic Compositions: Evidence from the Laney Member, Green River Formation, Wyoming. *Geol. Soc. America Bull.* 122, 236–252. doi:10.1130/b26522.1

Du, X. B., Liu, H., Liu, H. M., Lu, Y. C., Wang, Y., Hao, X. F., et al. (2016). Methods of Sequence Stratigraphy in the fine-grained Sediments: A Case from the Upper Fourth Sub-member and the Lower Third Sub-member of the Shahejie Formation in Well Fanye 1 of Dongying Depression. *Geol. Sci. Tech. Inf.* 35 (4), 1–11.

Egenhoff, S. O., and Fishman, N. S. (2013). Traces in the Dark--Sedimentary Processes and Facies Gradients in the Upper Shale Member of the Upper Devonian-Lower Mississippian Bakken Formation, Williston Basin, North Dakota, U.S.A. *J. Sediment. Res.* 83 (9), 803–824. doi:10.2110/jsr.2013.60

Elert, K., Sebastián Pardo, E., and Rodriguez-Navarro, C. (2015). Influence of Organic Matter on the Reactivity of clay Minerals in Highly Alkaline Environments. *Appl. Clay Sci.* 111, 27–36. doi:10.1016/j.clay.2015.03.006

Eugster, H. P., and Surdam, R. C. (1973). Depositional Environment of the Green River Formation of Wyoming: a Preliminary Report. *Geol. Soc. Am. Bull.* 84, 1115–1120.

Feng, Y., Jiang, S., Hu, S., Li, S., Lin, C., and Xie, X. (2016). Sequence Stratigraphy and Importance of Syndepositional Structural Slope-Break for Architecture of Paleogene Syn-Rift Lacustrine Strata, Bohai Bay Basin, E. China. *Mar. Pet. Geology.* 69, 183–204. doi:10.1016/j.marpetgeo.2015.10.013

Gou, Q., Xu, S., Hao, F., Yang, F., Zhang, B., Shu, Z., et al. (2019). Full-scale Pores and Micro-fractures Characterization Using FE-SEM, Gas Adsorption, Nano-CT and micro-CT: A Case Study of the Silurian Longmaxi Formation Shale in the Fuling Area, Sichuan Basin, China. *Fuel* 253, 167–179. doi:10.1016/j.fuel.2019.04.116

Gou, Q. Y., Xu, S., Hao, F., Yang, F., Shu, Z. G., and Liu, R. (2021). The Effect of Tectonic Deformation and Preservation Condition on the Shale Pore Structure Using Adsorption-Based Textural Quantification and 3D Image Observation. *Energy* 219, 11957. doi:10.1016/j.energy.2020.119579

Guo, J. H., Gong, S. B., and Wu, D. S. (1998). Sedimentary Sequence of the T-R Cycle and a Studied Example in the continental Fault Lacustrine Basin[J]. *Acta Sedimentologica Sinica* 16 (1), 8–14.

Hao, Y., Chen, F., Zhu, J., and Zhang, S. (2014). Reservoir Space of the Es 3 3 -Es 4 1 Shale in Dongying Sag. *Int. J. Mining Sci. Tech.* 24 (4), 425–431. doi:10.1016/j.ijmst.2014.05.002

He, J., Ding, W., Jiang, Z., Jiu, K., Li, A., and Sun, Y. (2017). Mineralogical and Chemical Distribution of the Es3L Oil Shale in the Jiyang Depression, Bohai Bay Basin (E China): Implications for Paleoenvironmental Reconstruction and Organic Matter Accumulation. *Mar. Pet. Geology.* 81, 196–219. doi:10.1016/j.marpetgeo.2017.01.007

Holditch, S. A. (2013). Unconventional Oil and Gas Resource Development - Let's Do it Right. *J. Unconventional Oil Gas Resour.* 1-2 (2), 2–8. doi:10.1016/j.juogr.2013.05.001

Ilgen, A. G., Heath, J. E., Akkutlu, I. Y., Bryndzia, L. T., Cole, D. R., Kharaka, Y. K., et al. (2017). Shales at All Scales: Exploring Coupled Processes in Mudrocks. *Earth-Science Rev.* 166, 132–152. doi:10.1016/j.earscirev.2016.12.013

Jia, J., Bechtel, A., Liu, Z., Strobl, S. A. I., Sun, P., and Sachsenhofer, R. F. (2013a). Oil Shale Formation in the Upper Cretaceous Nenjiang Formation of the Songliao Basin (NE China): Implications from Organic and Inorganic Geochemical Analyses. *Int. J. Coal Geology.* 113, 11–26. doi:10.1016/j.coal.2013.03.004

Jia, J., Liu, Z., Bechtel, A., Strobl, S. A. I., and Sun, P. (2013b). Tectonic and Climate Control of Oil Shale Deposition in the Upper Cretaceous Qingshankou Formation (Songliao Basin, NE China). *Int. J. Earth Sci. (Geol Rundsch)* 102, 1717–1734. doi:10.1007/s00531-013-0903-7

Jin, Z. K., Qi, C. W., Xue, J. Q., and Wang, C. S. (2006). Sedimentary Facies of the Jurassic in Northern Margin of Qaidam Basin. *J. Palaeogeogr.* 8, 199–210. doi:10.3969/j.issn.1671-1505.2006.02.006

Katz, B. J. (2003). Hydrocarbon Shows and Source Rocks in Scientific Ocean Drilling. *Int. J. Coal Geol.* 54 (1–2), 139–154. doi:10.1016/s0166-5162(03)00028-4

Kuhn, P. P., di Primio, R., Hill, R., Lawrence, J. R., and Horsfield, B. (2012). Three-dimensional Modeling Study of the Low-Permeability Petroleum System of the Bakken Formation. *Bulletin* 96 (10), 1867–1897. doi:10.1306/03261211063

Lazar, O. R., Bohacs, K. M., Macquaker, J. H. S., Schieber, J., and Demko, T. M. (2015). Capturing Key Attributes of Fine-Grained Sedimentary Rocks in Outcrops, Cores, and Thin Sections: Nomenclature and Description Guidelines. *J. Sediment. Res.* 85 (3), 230–246. doi:10.2110/jsr.2015.11

Lei, B., Que, H. P., Hu, N., Niu, Z. J., and Wang, H. (2002). Geochemistry and Sedimentary Environments of the Palaeozoic Siliceous Rocks in Western Hubei. *Sediment. Geol. Tethyan Geol.* 22, 70–79. doi:10.3969/j.issn.1009-3850.2002.02.010

Li, M. W., Jin, Z. Z., and Dong, M. Z. (2020b). Advances in the Basic Study of Lacustrine Shale Evolution and Shale Oil Accumulation. *Pet. Geology. Exp.* 48 (4), 408–505. doi:10.11781/sysydz202004489

Li, T., Jiang, Z., Xu, C., Liu, B., Liu, G., Wang, P., et al. (2017). Effect of Pore Structure on Shale Oil Accumulation in the Lower Third Member of the Shahejie Formation, Zhanhua Sag, Eastern China: Evidence from Gas Adsorption and Nuclear Magnetic Resonance. *Mar. Pet. Geology.* 88, 932–949. doi:10.1016/j.marpetgeo.2017.09.030

Li, W., Cao, J., Shi, C., Xu, T., Zhang, H., and Zhang, Y. (2020a). Shale Oil in saline Lacustrine Systems: A Perspective of Complex Lithologies of fine-grained Rocks. *Mar. Pet. Geology.* 116, 104351. doi:10.1016/j.marpetgeo.2020.104351

Li, X., Fan, Y. R., Deng, S. G., and Wang, T. S. (2009). Automatic Demarcation of Sequence Stratigraphy Using the Method of Well Logging Multiscale Data Fusion. *Pet. Exploration Dev.* 36 (02), 221–227. doi:10.3321/j.issn:1000-0747.2009.02.013

Liang, C., Cao, Y., Jiang, Z., Wu, J., Guoqi, S., and Wang, Y. (2017). Shale Oil Potential of Lacustrine Black Shale in the Eocene Dongying Depression: Implications for Geochemistry and Reservoir Characteristics. *Bulletin* 101, 1835–1858. doi:10.1306/01251715249

Liang, C., Wu, J., Jiang, Z., Cao, Y., and Song, G. (2018). Sedimentary Environmental Controls on Petrology and Organic Matter Accumulation in the Upper Fourth Member of the Shahejie Formation (Paleogene, Dongying Depression, Bohai Bay Basin, China). *Int. J. Coal Geology.* 186, 1–13. doi:10.1016/j.coal.2017.11.016

Liu, B., Shi, J. X., Fu, X. F., Lü, Y. F., Sun, X. D., Gong, L., et al. (2018a). Petrological Characteristics and Shale Oil Enrichment of Lacustrine fine-grained Sedimentary System: A Case Study of Organic-Rich Shale in First Member of Cretaceous Qingshankou for Mation in Gulong Sag, Songliao Basin, NE China[J]. *Pet. Exploration Dev.* 45 (5), 828–838. doi:10.1016/s1876-3804(18)30091-0

Liu, B., Song, Y., Zhu, K., Su, P., Ye, X., and Zhao, W. (2020). Mineralogy and Element Geochemistry of Salinized Lacustrine Organic-Rich Shale in the Middle Permian Santanghu Basin: Implications for Paleoenvironment, Provenance, Tectonic Setting and Shale Oil Potential. *Mar. Pet. Geology.* 120, 104569. doi:10.1016/j.marpetgeo.2020.104569

Liu, H., Zhang, S., Song, G., Xuejun, W., Teng, J., Wang, M., et al. (2019a). Effect of Shale Diagenesis on Pores and Storage Capacity in the Paleogene Shahejie Formation, Dongying Depression, Bohai Bay Basin, east China. *Mar. Pet. Geology.* 103, 738–752. doi:10.1016/j.marpetgeo.2019.01.002

Liu, Z., Algeo, T. J., Guo, X., Fan, J., Du, X., and Lu, Y. (2017). Paleo-environmental Cyclicity in the Early Silurian Yangtze Sea (South China): Tectonic or Glacio-Eustatic Control. *Palaeogeogr. Palaeoclimatol. Palaeoecol.* 466, 59–76. doi:10.1016/j.palaeo.2016.11.007

Liu, Z. B., Liu, G. X., and Hu, Z. Q. (2019b). Lithofacies Types and Assemblage Features of continental Shale Strata and Their Significance for Shale Gas Exploration: A Case Study of the Middle and Lower Jurassic Strata in the Sichuan Basin. *Pet. Geology. Exp.* 39 (12), 10–21.

Liu, Z., Huang, C., Algeo, T. J., Liu, H., Hao, Y., Du, X., et al. (2018b). High-resolution Astrochronological Record for the Paleocene-Oligocene (66-23 Ma) from the Rapidly Subsiding Bohai Bay Basin, Northeastern China. *Palaeogeogr. Palaeoclimatol. Palaeoecol.* 510, 78–92. doi:10.1016/j.palaeo.2017.10.030

Loucks, R. G., Ruppel, S. C., and Mississippian, B. S. (2007). Mississippian Barnett Shale: Lithofacies and Depositional Setting of a Deep-Water Shale-Gas Succession in the Fort Worth Basin, Texas. *Bulletin* 91 (4), 579–601. doi:10.1306/11020606059

Lu, Y., Jiang, S., Lu, Y., Xu, S., Shu, Y., and Wang, Y. (2019). Productivity or Preservation? the Factors Controlling the Organic Matter Accumulation in the Late Katian through Hirnantian Wufeng Organic-Rich Shale, South China. *Mar. Pet. Geology.* 109, 22–35. doi:10.1016/j.marpetgeo.2019.06.007

Ma, B., Cao, Y., Eriksson, K. A., Jia, Y., and Wang, Y. (2016). Burial Evolution of Evaporites with Implications for Sublacustrine Fan Reservoir Quality: a Case Study from the Eocene Es4x Interval, Dongying Depression, Bohai Bay Basin, China. *Mar. Pet. Geology.* 76, 98–114. doi:10.1016/j.marpetgeo.2016.05.014

Ma, Y. Q., Du, X. B., Liu, H. M., and Lu, Y. C. (2017). Characteristics, Depositional Processes, and Evolution of Shale Lithofacies of the Upper Submember of E2s4 in the Dongying Depression[J]. *Earth Sci.* 42 (7), 1195–1208. doi:10.3799/dqkx.2017.097

Ma, Y. Q., Liu, H. M., and Zhang, S. P. (2020). Types of Fine-Grained Mixed Sedimentary Rocks of Shahejie Formation and Evolution of Lake Basin in Jiyang Depression, Eastern China. *Earth Sci.* 45 (10), 3633–3644. doi:10.3799/dqkx.2020.192

Macquaker, J. H. S., Keller, M. A., and Davies, S. J. (2010). Algal Blooms and "Marine Snow": Mechanisms that Enhance Preservation of Organic Carbon in Ancient Fine-Grained Sediments. *J. Sediment. Res.* 80 (11), 934–942. doi:10.2110/jsr.2010.085

Meng, Q., Liu, Z., Bruch, A. A., Liu, R., and Hu, F. (2012). Palaeoclimatic Evolution during Eocene and its Influence on Oil Shale Mineralisation, Fushun basin, China. *J. Asian Earth Sci.* 45, 95–105. doi:10.1016/j.jseaes.2011.09.021

Merkel, A., Fink, R., and Littke, R. (2016). High Pressure Methane Sorption Characteristics of Lacustrine Shales from the Midland Valley Basin, Scotland. *Fuel* 182, 361–372. doi:10.1016/j.fuel.2016.05.118

Mitra, A., Warrington, D. S., and Sommer, A. (2010). "Application of Lithofacies Models to Characterize Unconventional Shale Gas Reservoirs and Identify Optimal Completion Intervals," in Proceedings of SPE Western Regional Meeting in Anaheim. California,USA. May, 27-29 2010. [C]. paper SPE 132513.

Ortiz Cancino, O. P., Peredo Mancilla, D., Pozo, M., Pérez, E., and Bessieres, D. (2017). Effect of Organic Matter and thermal Maturity on Methane Adsorption Capacity on Shales from the Middle magdalena Valley Basin in Colombia. *Energy Fuels* 31 (11), 11698–11709. doi:10.1021/acs.energyfuels.7b01849

Ougier-Simonin, A., Renard, F., Boehm, C., and Vidal-Gilbert, S. (2016). Microfracturing and Microporosity in Shales. *Earth-Science Rev.* 162, 198–226. doi:10.1016/j.earscirev.2016.09.006

Ross, D., and Bustin, R. (2009). Investigating the Use of Sedimentary Geochemical Proxies for Paleoenvironment Interpretation of Thermally Mature Organic-Rich Strata: Examples from the Devonian–Mississippian Shales, Western Canadian Sedimentary Basin. *Chem. Geol.* 260 (1–2), 1–19. doi:10.1016/j.chemgeo.2008.10.027

Sageman, B. B., Murphy, A. E., Werne, J. P., Ver Straeten, C. A., Hollande, D. J., and Lyons, T. W. (2003). A Tale of Shales: The Relative Roles of Production, Decomposition, and Dilution in the Accumulation of Organic Rich Strata, Middle Upper Devonian, Appalachian Basin. *Chem. Geology.* 195 (1), 229–273. doi:10.1016/s0009-2541(02)00397-2

Scherer, C. M. S., Goldberg, K., and Bardola, T. (2015). Facies Architecture and Sequence Stratigraphy of an Early post-rift Fluvial Succession, Aptian Barbalha Formation, Araripe Basin, Northeastern Brazil. *Sediment. Geology.* 322, 43–62. doi:10.1016/j.sedgeo.2015.03.010

Shi, J., Jin, Z., Liu, Q., Zhang, R., and Huang, Z. (2019a). Cyclostratigraphy and Astronomical Tuning of the Middle Eocene Terrestrial Successions in the Bohai Bay Basin, Eastern China. *Glob. Planet. Change* 174, 115–126. doi:10.1016/j.gloplacha.2019.01.001

Shi, J. Y., Jin, Z. J., Liu, Q. Y., and Huang, Z. (2019b). Depositional Process and Astronomical Forcing Model of Lacustrine fine-grained Sedimentary Rocks: a Case Study of the Early Paleogene in the Dongying Sag, Bohai Bay Basin. *Mar. Petrol. Geol.* 113, 103995. doi:10.1016/j.marpetgeo.2019.08.023

Smith, M. E., Carroll, A. R., Scott, J. J., and Singer, B. S. (2014). Early Eocene Carbon Isotope Excursions and Landscape Destabilization at Eccentricity Minima: Green River Formation of Wyoming. *Earth Planet. Sci. Lett.* 403, 393–406. doi:10.1016/j.epsl.2014.06.024

Strobl, S. A. I., Sachsenhofer, R. F., Bechtel, A., Gratzer, R., Gross, D., Bokhari, S. N. H., et al. (2014). Depositional Environment of Oil Shale within the Eocene Jijuntun Formation in the Fushun Basin (NE China). *Mar. Pet. Geology.* 56, 166–183. doi:10.1016/j.marpetgeo.2014.04.011

Su, S., Jiang, Z., Shan, X., Ning, C., Zhu, Y., Wang, X., et al. (2019). Effect of Lithofacies on Shale Reservoir and Hydrocarbon Bearing Capacity in the Shahejie Formation, Zhanhua Sag, Eastern China. *J. Pet. Sci. Eng.* 174, 1303–1308. doi:10.1016/j.petrol.2018.11.048

Sun, P., Sachsenhofer, R. F., Liu, Z., Strobl, S. A. I., Meng, Q., Liu, R., et al. (2013). Organic Matter Accumulation in the Oil Shale- and Coal-Bearing Huadian Basin (Eocene; NE China). *Int. J. Coal Geology.* 105, 1–15. doi:10.1016/j.coal.2012.11.009

Surdam, R. C., and Stanley, K. O. (1979). Lacustrine Sedimentation During the Culminating Phase of Eocene Lake Gosiute, Wyoming (Green River Formation). *Geol. Soc. Am. Bull.* 90, 93–110. doi:10.1130/0016-7606(1979)90<93:LSDTCP>2.0.CO;2

Tribovillard, N. (2006). Organic Facies Variation in the Late Kimmeridgian of the Boulonnais Area (Northernmost France). *Marine Petrol. Geol.* 18, 371–389.

Vosoughi Moradi, A., Sarı, A., and Akkaya, P. (2016). Paleoredox Reconstruction of Bituminous Shales from the Miocene Hançili Formation, Çankırı-Çorum Basin, Turkey: Evaluating the Role of Anoxia in Accumulation of Organic-Rich Shales. *Mar. Pet. Geology.* 78, 136–150. doi:10.1016/j.marpetgeo.2016.09.012

Wang, H. (2007). *The Basic Principles and Application Methods of Sequence stratigrap[M]*. Wuhan. China University of Geosciences Press, 1–3.

Wang, Y., Xu, S., Hao, F., Lu, Y., Shu, Z., Yan, D., et al. (2018). Geochemical and Petrographic Characteristics of Wufeng-Longmaxi Shales, Jiaoshiba Area, Southwest China: Implications for Organic Matter Differential Accumulationerential Accumulation. *Mar. Pet. Geology.* 102, 138–154. doi:10.1016/j.marpetgeo.2018.12.038

Wu, Z. Y., Zhao, X. Z., and Wang, E. (2020). Sedimentary Environment and Organic Enrichment Mechanisms of Lacustrine Shale: A Case Study of the Paleogene Shahejie Formation, Qikou Sag, Bohai Bay Basin. *Palaeogeography, Palaeoclimatology, Palaeoecology* 573, 110404. doi:10.1016/j.palaeo.2021.110404

Xu, J., Liu, Z., Bechtel, A., Meng, Q., Sun, P., Jia, J., et al. (2015). Basin Evolution and Oil Shale Deposition during Upper Cretaceous in the Songliao Basin (NE China): Implications from Sequence Stratigraphy and Geochemistry. *Int. J. Coal Geology.* 149, 9–23. doi:10.1016/j.coal.2015.07.005

Xu, S., Gou, Q., Hao, F., Zhang, B., Shu, Z., Lu, Y., et al. (2020a). Shale Pore Structure Characteristics of the High and Low Productivity wells, Jiaoshiba Shale Gas Field, Sichuan Basin, China: Dominated by Lithofacies or Preservation Condition. *Mar. Pet. Geology.* 114, 104211. doi:10.1016/j.marpetgeo.2019.104211

Xu, S., Hao, F., Shu, Z., Zhang, A., and Yang, F. (2020b). Pore Structures of Different Types of Shales and Shale Gas Exploration of the Ordovician Wufeng and Silurian Longmaxi Successions in the Eastern Sichuan Basin, South China. *J. Asian Earth Sci.* 193, 104271. doi:10.1016/j.jseaes.2020.104271

Yan, L., and Zheng, M. (2015). The Response of lake Variations to Climate Change in the Past Forty Years: a Case Study of the Northeastern Tibetan Plateau and Adjacent Areas, China. *Quat. Int.* 371, 31–48. doi:10.1016/j.quaint.2014.12.057

Yang, J. M., Huang, B. G., Liu, W. L., Gao, Z. N., and Li, J. F. (2019). Quantitative Division of High Resolution Sequence Stratigraphy in Shallow Water delta Based on Wavelet Transform. *J. Yangtze Univ. (Natural Sci. Edition)* 16 (12), 20–24. doi:10.16772/j.cnki.1673-1409.2019.12.004

Yang, T., Cao, Y., Friis, H., Wang, Y., and Zhou, L. (2018). Diagenetic Evolution and Chemical Changes of Deep-Water Mudstones of Shahejie Formation in the Dongying Sag, Jiyang Depression, Eastern China. *Mar. Pet. Geology.* 93, 14–32. doi:10.1016/j.marpetgeo.2018.02.005

Zhang, J. C., Lin, L. M., Li, Y. X., Tang, X., Zhu, L. L., and Xin, Y. W. (2012). Classification and Evaluation of Shale Oil[J]. *Earth Sci. Front.* 19 (5), 322–331.

Zhang, L., Chen, Z., Li, Z., Zhang, S., Li, J., Liu, Q., et al. (2019a). Structural Features and Genesis of Microscopic Pores in Lacustrine Shale in an Oil Window: a Case Study of the Dongying Depression. *Bulletin* 103 (8), 1889–1924. doi:10.1306/1218181522717084

Zhang, S., Liu, H. M., Chen, S. Y., Wang, Y. S., Pu, X. G., Zhang, K. H., et al. (2017). Classification Scheme for Lithofacies of Finegrained Sedimentary Rocks in Faulted Basins of Eastern China: Insights from the fine-grained Sedimentary Rocks in Paleogene, Southern Bohai Bay Basin[J]. *Acta Geologica Sinica* 91 (5), 1108–1119.

Zhang, S., Liu, H. M., Liu, Y. L., Wang, Y. S., Wang, M., and Bao, Y. S. (2019b). Main Controls and Geological Sweet Spot Types in Paleogene Shale Oil Rich Areas of the Jiyang Depression, Bohai Bay basin, China. *Mar. Petrol. Geol.* 111, 576–587. doi:10.1016/j.marpetgeo.2019.08.054

Zhao, D. F., Guo, H. Y., Wang, G., Li, G. L., Zeng, C. L., and Jiao, W. W. (2020). Sequence Stratigraphic Framework and its Influence on the Development Characteristics of Shale Reservoirs: Taking the Longmaxi Formation Shale in the Sichuan Basin as an Example. *Acta Sedimentologica Sinica* 38 (02), 379–397. doi:10.14027/j.issn.1000-0550.2019.043

Zou, C. (2017). "Shale Oil and Gas," in *Unconventional Petroleum Geology*. 2nd ed. (Elsevier), 275–321. doi:10.1016/b978-0-12-812234-1.00010-8

Zou, C., Yang, Z., Zhu, R., Wu, S., Fu, J., Lei, D., et al. (2019). Geologic Significance and Optimization Technique of Sweet Spots in Unconventional Shale Systems. *J. Asian Earth Sci.* 178, 3–19. doi:10.1016/j.jseaes.2018.07.005

Conflict of Interest: Authors YS, HB, YZ, MC, HL, WP, and LZ were employed by the company Sinopec Jianghan Oilfield Company.

The remaining authors declare that the research was conducted in the absence of any commercial or financial relationships that could be construed as a potential conflict of interest. This study received funding from the Research Institute of Exploration and Development, SINOPEC Jianghan Oilfield Company. The funder had the following involvement in the study: study design, data collection and analysis, decision to publish, and preparation of the manuscript.